Hydrologic Conceptualization of San Solomon Springs in the Lower Delaware Basin

Prepared for:

Big Bend Conservation Alliance

By:

Rebecca R. Nunu and Ronald T. Green, Ph.D., P.G.

May 24, 2021
Final Report

SwRI®
Southwest Research Institute

Project scope and description

The San Solomon Springs system in semi-arid west Texas is a multi-outlet spring system with potentially different source areas for each spring. The spring system includes San Solomon (otherwise known as Balmorhea State Park), Phantom Lake, Giffin, East Sandia, West Sandia, and Saragosa springs. Conceptualization of each spring's source area (i.e., source of recharge) is not well understood, which raises concern as demand for water continues to increase and future pumping or decreased recharge from changing precipitation patterns could affect spring quality and quantity.

The geochemical assemblage of any spring, river, or groundwater sample comprises isotopes, ions, and field parameters. Collectively, these constituents imprint water with a geochemical "fingerprint" that can distinguish it from other waters with different histories or flow paths. Geochemical signatures have provided a strong basis to conceptualize the regional flow system in Trans-Pecos Texas. San Solomon, Phantom Lake, and Giffin springs have been previously studied extensively within the context of this regional flow system. However, these advances do not include a detailed understanding of East Sandia, West Sandia, or Saragosa springs nor local flow effects that may contribute to all six springs. The research objective of this study is to investigate the hydraulic relationships among the six individual springs of San Solomon Springs using geochemical and statistical analyses.

A Jacob and Terese Hershey Foundation grant was awarded to Southwest Research Institute® (SwRI) to conduct a geochemical investigation of spring waters to refine the delineation of source areas to this multi-outlet spring system. The award allowed the project team to collect and analyze water samples from the six springs and from three groundwater wells set in different aquifers in the study area. These robust data were synthesized and interpreted using cross plots of geochemical constituents, geochemical equilibria calculations, and multivariate statistical analyses. This approach, when coupled with an improved understanding of the geological structural framework in the region, highlighted nuanced variations in the geochemical data to refine and constrain previously outlined source areas to each individual spring of the San Solomon Springs system. In doing so, the following research question was addressed: do different local and/or regional sources contribute to the six springs of San Solomon Springs? The results of this project suggest that at least four source areas contribute to San Solomon Springs.

Attainment of goals

As part of this phase of work, water samples were collected and analyzed from the six springs in the San Solomon Springs system and three wells in aquifers within the study area: the Cenozoic Pecos Alluvial Aquifer, the Edwards-Trinity Aquifer (Upper Cretaceous), and the Igneous Aquifer (Tertiary Volcanics) (Figure 1). Chemical analyses included field parameters (i.e., pH, temperature, specific conductivity), major cations and anions (i.e., calcium, magnesium, sodium, potassium, chloride, bicarbonate, sulfate, nitrate, strontium), and isotopes (i.e., deuterium, tritium, carbon-

13/14, oxygen-18, sulfur-34, strontium-87, boron-11). Analysis results were complemented by data and analysis provided as part of previous phases of work conducted by the SwRI project team at the spring system. These expanded data sets allowed for assessment of temporal variability in spring discharge composition.

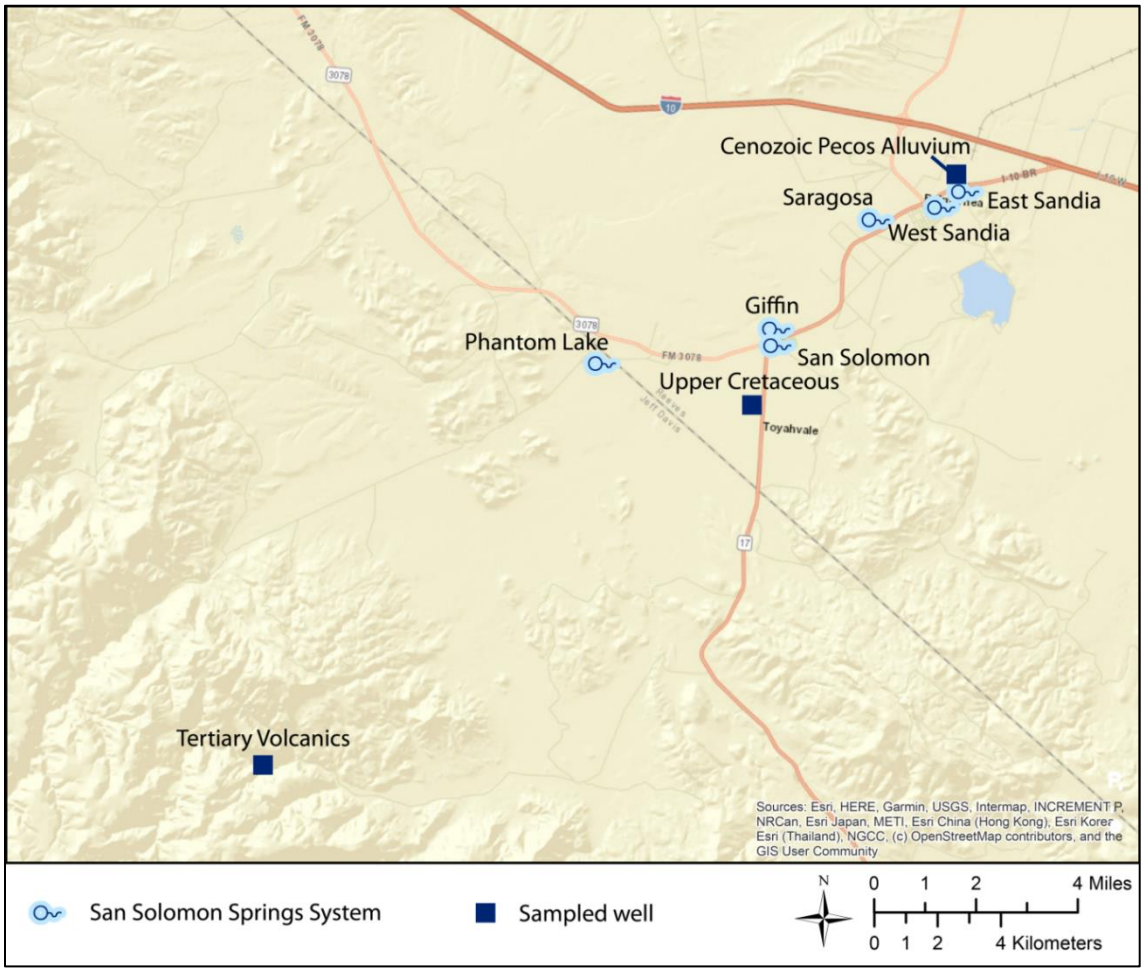

Figure 1. Spring and well sample locations.

This comprehensive set of water chemistry analyses provided the foundation to explore the relationships among the water groupings and how the relationships vary with time. These geochemical and statistical analyses and ensuing interpretations allowed for improved and enhanced understanding of the relationships among the six springs in the San Solomon Springs system, the primary research goal of the project.

Outcome measurements

Goals attained as a result of this project allowed for the identification of different sources to the San Solomon Springs system, and the interpretation of relationships among water groupings using geochemical and multivariate statistical analyses. Despite seemingly similar hydrochemical assemblages in all six springs, in-depth scrutiny of the plots of ion chemistry and isotopic

compositions and multivariate statistical analyses support the notion that there are at least four different flow components that contribute to the springs (Figure 2):

1) The main component is regional flow through carbonate rocks that upwell through the Edwards-Trinity Aquifer and Cenozoic Pecos Alluvium at the springs (purple box).
2) Infiltration through the Cenozoic Pecos Alluvium that is added by either irrigation return flow or precipitation and recharges East Sandia and West Sandia springs (blue box).
3) An irrigation or precipitation component near Saragosa Spring contributes to its springflow (gray box).
4) Local precipitation enters the regional system and discharges at the springs (blue boxes).

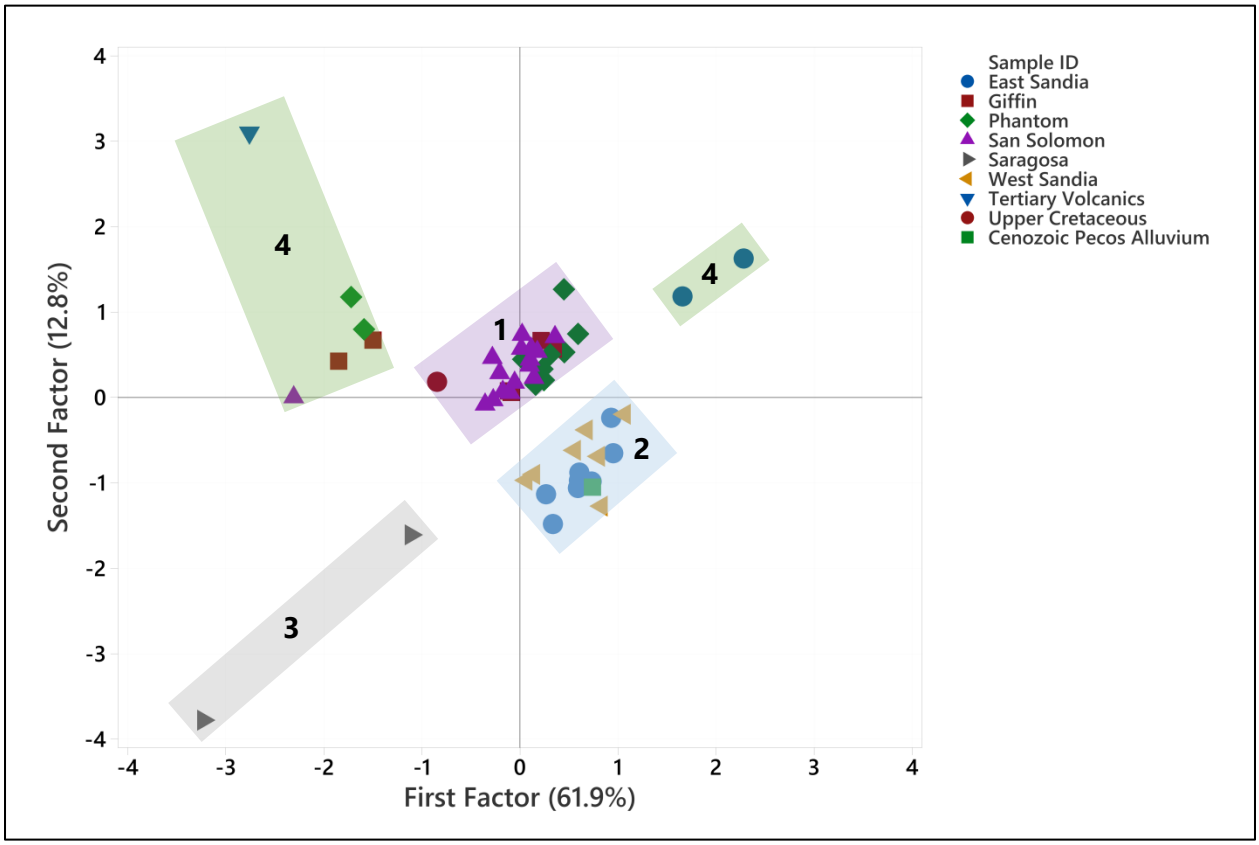

Figure 2. Results from multivariate statistical analysis that effectively separates the spring and well hydrochemistry by source area.

The outcome of this study elucidates four source areas of recharge that sustain San Solomon Springs. As described in greater detail under "Lessons Learned", the results suggest that the main source of recharge to the six springs mostly comes from the northwest. However, groundwater extraction from adjoining areas to provide for increasing water demands could impact spring discharge depending on actual locations and rates of pumping of extraction wells. Water resource managers and vested stakeholders can use this refined conceptual model to monitor source area 1 that may be developed for groundwater pumping and impact the springs. Source areas 2-4 are surficial recharge sources that would not impacted by deep groundwater pumping as much as source area 1.

Details of the technical approach and the robust analysis of hydrochemical data used to delineate the different source areas to San Solomon Springs are included in the December 2020 Interim Status Report (Appendix A).

Lessons learned

The motivation for this project was to evaluate the potential impact of unconventional oil and gas development on the quantity and quality of discharge from the springs in the San Solomon Springs system. Subsequent to the onset of this multi-phase effort, the unconventional oil and gas activities that were anticipated at that time were curtailed and have since been abandoned. Nonetheless, the source areas to San Solomon Springs identified in this refined conceptualization remain the potential target of other stressors and demands (e.g., municipal and irrigation water use, changes in precipitation) in addition to other unconventional oil/gas development that could impact spring discharge if the groundwater withdrawals occur in the source areas to the springs (Figure 3).

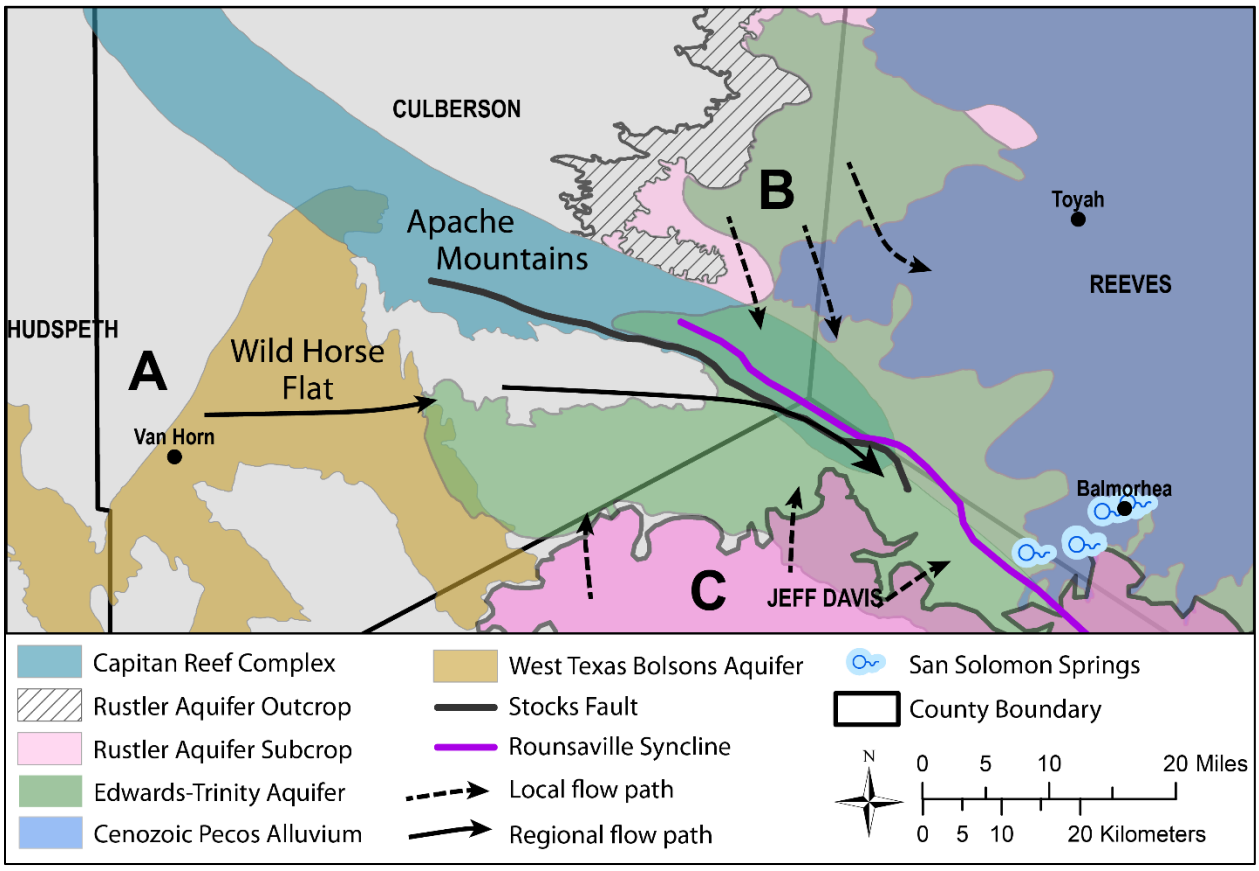

Figure 3. Sources of recharge to the springs (illustrated by local and regional flow paths – see Appendix A).

Threats to the springs remain. In particular, extraction of groundwater from the source areas that sustain the springs could deplete the springflow if excessive pumping is experienced. It is important to focus future investigations on areas from which water may be extracted to support growing demands. The project team recommends additional investigations of areas to the

northwest of the San Solomon Springs system near the Culberson/Jeff Davis/Reeves-county intersection (Figure 3).

Lessons learned during this project included the following:

1) Analysis of the water chemistry of spring discharge supports the hypothesis that source areas vary among the springs.
2) Discharge quantity and quality from the springs varies over time in response to drought, recharge events (i.e., precipitation), irrigation practices, and groundwater pumping.
3) Source areas to all six springs are generally west and northwest of the springs.
4) Although unconventional oil and gas development is not a current threat to the springs, development of water well fields in the source areas located upgradient and west of the springs could be detrimental to the future viability of the springs (Figure 3). Of particular concern is development of groundwater well fields near the common borders of Culberson, Reeves, and Jeff Davis counties.

Unspent funds

All funds from the awarded grant have been spent to fulfill the project tasks.

Appendix: Interim Status Report

Hydrologic Conceptualization of San Solomon Springs in the Lower Delaware Basin

Prepared for:

Big Bend Conservation Alliance

By:

Rebecca R. Nunu and Ronald T. Green, Ph.D., P.G.

December 29, 2020

Status Report

SwRI
SOUTHWEST RESEARCH INSTITUTE

Executive Summary

Effective water management requires that source areas to springs in arid and semi-arid environments be characterized well enough to assess impacts on flow from changes in recharge and groundwater withdrawals. Geochemical signatures of groundwater can be used as indicators of different components of flow to springs and can be especially useful for characterizing different sources that contribute to multi-outlet spring systems. San Solomon Springs in Trans-Pecos Texas provides an example of a multi-outlet spring system with potentially different source areas. Samples from each of the six named orifices at San Solomon Springs were collected in 2019 and 2020 and combined with historical data to assess the geochemical signatures of the spring system. Results of analyses of field parameters, ions and trace elements, and multiple stable and radiogenic isotopes were combined with multivariate statistical analyses (principal component and exploratory factor analyses) to investigate the hydraulic relationships among the individual springs of San Solomon Springs.

Results show that all six spring outlets are represented by Na-Cl-SO_4 hydrochemical facies. Isotopic compositions of all six springs are consistent with a conceptual model of older groundwater (likely of Pleistocene age) from a regional flow system that upwells through carbonates and alluvial sediments to discharge at the springs. Elevated ion concentrations and carbon isotopes in East Sandia and West Sandia springs indicate infiltration of water, added by either irrigation return flow or precipitation, through alluvial sediments adds to flows at both spring outlets. Saragosa Spring is likely a seepage spring and is more heavily influenced by a near surface component (e.g., irrigation or precipitation). A subset of records for San Solomon, Phantom Lake, and Giffin springs indicating elevated ^{3}H and NO_3^- and lower ion concentrations suggest precipitation also enters the regional system as local recharge. Statistical analyses using major ion chemistry alone effectively identify as many as four different flow components to the spring system. Isotopic and trace element data complement the statistical analyses and are consistent with multiple sources of flow to the springs.

Table of Contents

List of Figures

List of Tables

Introduction

San Solomon Springs is situated in Trans-Pecos Texas, the semi-arid region west of the Pecos River and east of the Rio Grande (Figure 1). Surface water is quite limited in this region. San Solomon Springs includes six named springs: San Solomon, Giffin, Saragosa, West Sandia, and East Sandia springs discharge in Reeves County, and Phantom Lake Spring discharges along the Jeff Davis and Reeves County border near Toyahvale, Texas (Figure 2). San Solomon, Phantom Lake, and Giffin springs have been classified as artesian springs whereas Saragosa, East Sandia, and West Sandia springs have been classified as gravity springs (White et al., 1941). The spring system provides for recreation, irrigation, and municipal water purposes for the community in Balmorhea, Texas and neighboring areas. The springs also provide habitats for rare and endemic species found in San Solomon, Phantom Lake, and East Sandia Springs. Federally endangered species that depend on these spring habitats include the Comanche Springs pupfish and Pecos gambusia (TPWD, 2018).

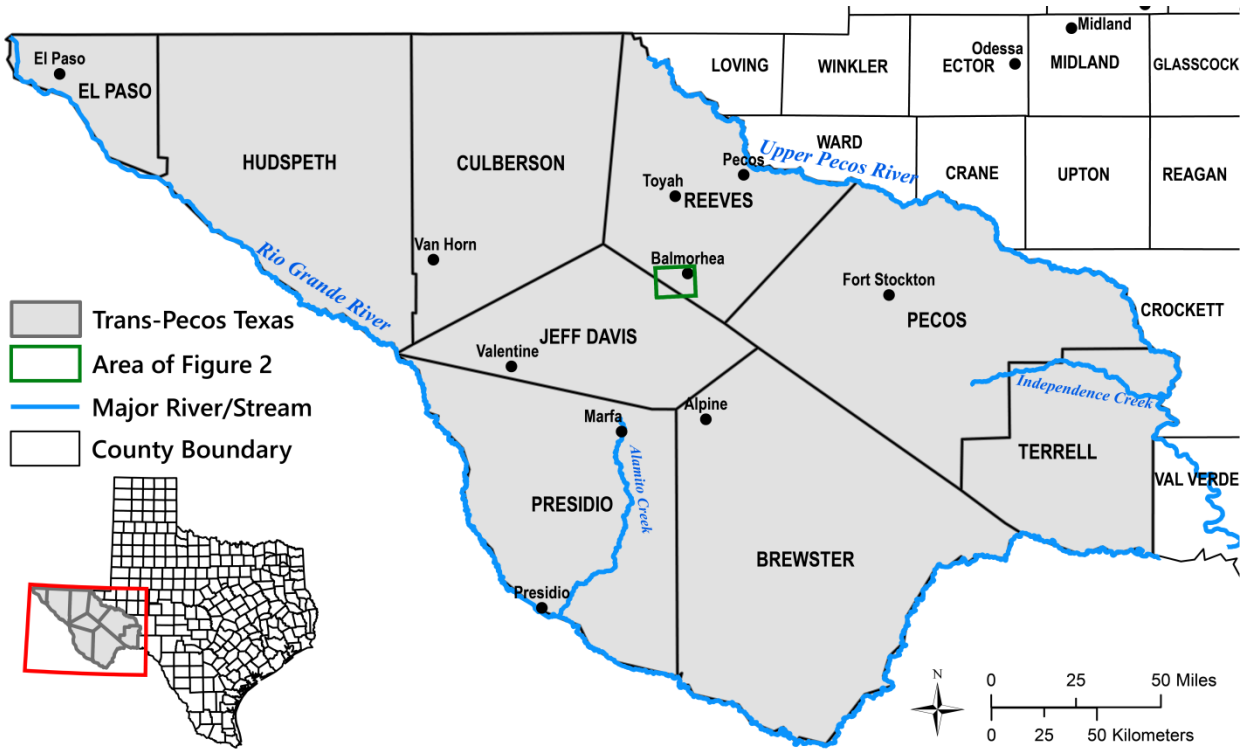

Figure 1. Location of Trans-Pecos Texas.

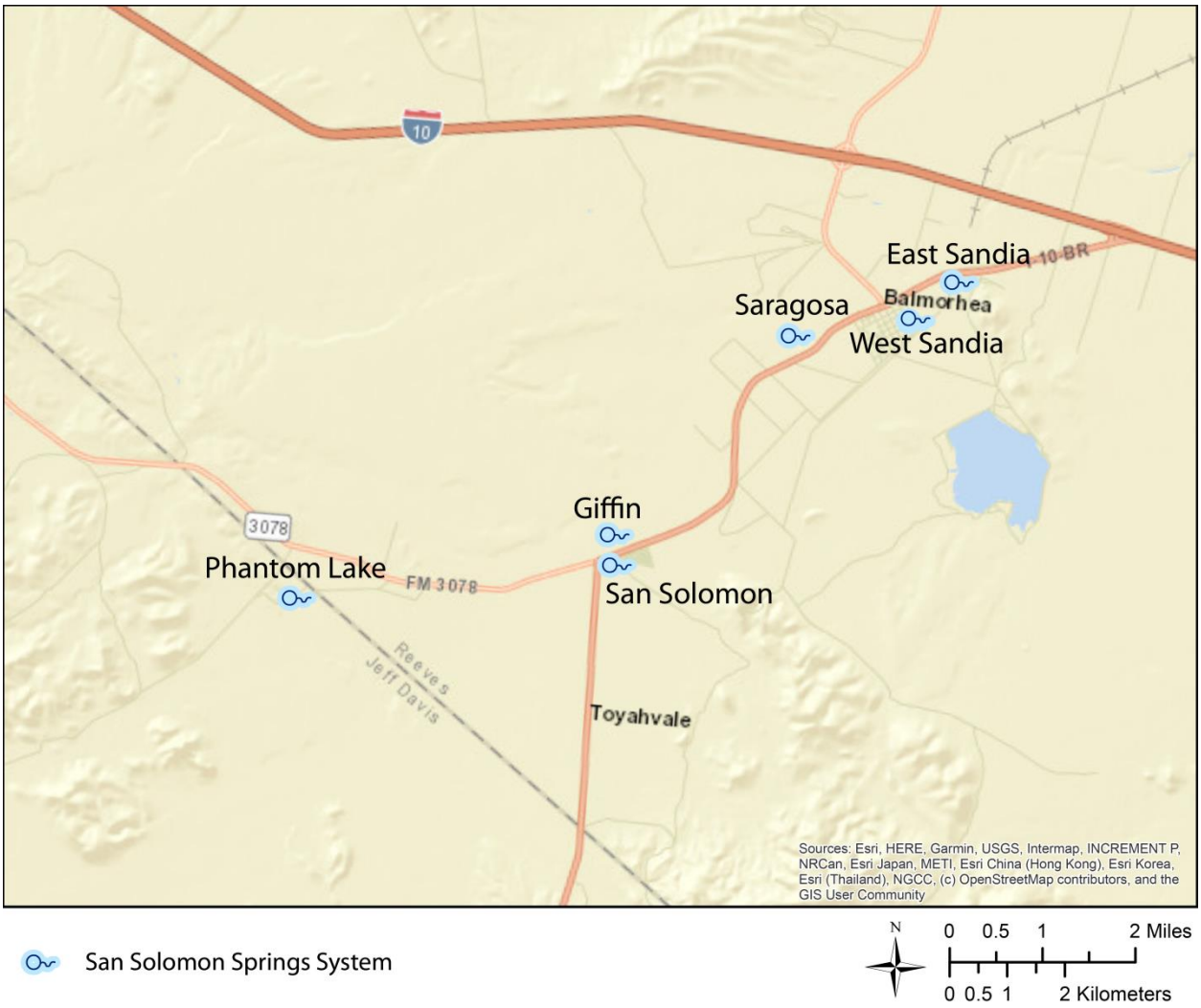

Figure 2. Location of San Solomon Springs.

San Solomon Springs in west-central Texas provides an example of a multi-outlet spring system with potentially different source areas for the springs. Previous studies have established that multiple source areas contribute to spring discharge in the San Solomon Springs system (White et al., 1941; LaFave and Sharp, 1987; Uliana et al., 2007). Uliana et al. (2007) used multi-isotope analysis to identify three sources that contribute to the regional flow system in Trans-Pecos Texas and ultimately discharge at San Solomon Springs (Figure 3). Stable isotopes indicate that recharge to this regional groundwater flow system includes water that originated in Wild Horse Flat during a cooler and wetter climatic period in the Pleistocene. Endmember A identified by Uliana et al. (2007) is characterized by low total dissolved solids (TDS) and high $^{87}Sr/^{86}Sr$ waters originating from Wild Horse Flat. Endmember B is from the Rustler Aquifer and is characterized by high TDS water with a distinct geochemical signature that suggests anhydrite dissolution. Low TDS and median $^{87}Sr/^{86}Sr$ waters characterize Endmember C which originates in the Davis

Mountains. These sources of recharge flow along faults and fractures through the Edwards-Trinity Aquifer and discharge at the springs.

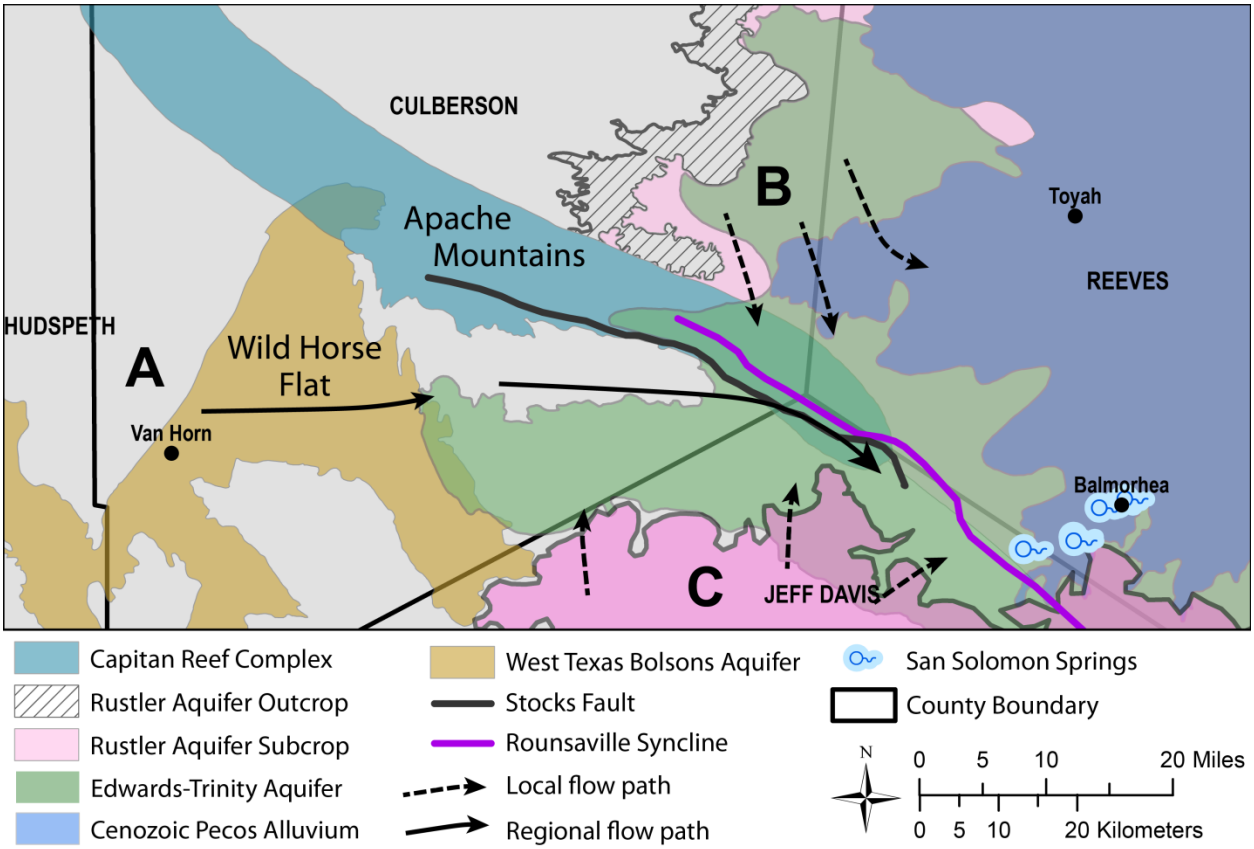

Figure 3. Regional groundwater flow paths near Balmorhea, Texas discerned using a multi-isotope approach (modified from Uliana et al. (2007)). Flow paths illustrate the complexity of multiple source areas discharging to multiple spring outlets.

Groundwater geochemical signatures have provided a strong basis to conceptualize the regional flow system in Trans-Pecos Texas. San Solomon, Phantom Lake, and Giffin springs have been studied extensively within the context of this regional flow system. However, these advances do not account for a detailed understanding of East Sandia, West Sandia, or Saragosa springs nor local flow effects that may contribute to the springs. This raises concern as the ubiquitous demand for water resources in this semi-arid environment continues to increase. The impact of pumping on spring discharge cannot be determined if source areas to springs are unknown. The research objective of this study is to investigate the hydraulic relationships among the six individual springs of San Solomon Springs using geochemical and statistical analyses. The following research question is addressed: do different local and/or regional sources contribute to the six springs of San Solomon Springs? In doing so, this study aims to ascertain if natural tracers that build groundwater geochemical signatures are representative of different sources that contribute to the complex (multi-source, multi-outlet) spring system.

Geochemical assessments

The geochemical assemblage of any spring, river, or groundwater sample comprises isotopes, ions, and trace elements. Collectively, these geochemical constituents leave water with a hydrochemical "fingerprint" that can distinguish it from other waters with different histories or flow paths (Ladouche et al., 2001). Such constituents include water temperature, specific conductance, pH, and dissolved oxygen whose variance over time and space can provide insight on flow regimes (Birk et al., 2004; Ravbar et al., 2011). Ions and trace elements are insightful of source rock interactions as water picks up these constituents, and consequently source rock signatures, along flow paths. Major cations used to identify source rock interactions include calcium (Ca^{2+}), magnesium (Mg^{2+}), sodium (Na^{+}), potassium (K^{+}), lithium (Li^{+}), strontium (Sr^{2+}) boron (B^{3+}), and ammonium (NH_4^{+}). Conversely, major anions include sulfate (SO_4^{2-}), chloride (Cl^{-}), fluoride (F^{-}), bromide (Br^{-}), nitrate (NO_3^{-}), and phosphate (PO_4^{3-}). Bicarbonate (HCO_3^{-}) is another major ion that most often contributes to alkalinity. Dissolved silica (SiO_2 (aq)) in natural waters is derived from the chemical weathering of silicate minerals in host rocks (Hem, 1985).

Isotopes can be characterized as either stable or radiogenic. Both stable and radiogenic isotopes are commonly used and well-established as key discriminators in groundwater studies. Elements with stable isotopes commonly used in hydrologic studies include hydrogen, oxygen, and carbon (Bullen and Kendall, 1998; Doctor et al., 2006; Mance et al., 2014). Variations in the ratios of stable isotopes of an element are a function of isotopic fractionation. Heavy and light isotopes may partition differently due to various kinetic or biological processes because of their mass difference. Thus, isotopes tend to act in a biased manner (fractionate) during environmental and hydrologic processes such as evaporation and condensation. Low mass stable isotopic compositions are expressed as ratio of an element's heavier isotope to its lighter isotope. The delta notation "δ" is used to express this isotopic ratio relative to a reference standard in parts per thousand (‰). For example, the isotopic ratio of oxygen, $\delta^{18}O$, is equivalent to $^{18}O/^{16}O$. This ratio is expressed relative to VSMOW (Vienna Standard Mean Ocean Water).

Isotopic ratios of hydrogen ($\delta^{2}H$) and oxygen ($\delta^{18}O$) tend to act in a biased manner during hydrologic processes such as evaporation and condensation. The Global Meteoric Water Line (GMWL) describes the average relationship between $\delta^{2}H$ and $\delta^{18}O$ observed in natural meteoric waters (Craig, 1961). This relationship, $\delta^{2}H = 10 + 8*\delta^{18}O$, can be used to ascertain origins of water, namely altitude, continental, and latitude effects present at the time of recharge.

Carbon-13 ($\delta^{13}C$) of Dissolved Inorganic Carbon (DIC) in water can distinguish between sources of carbon due to microbial activities, vegetation, and carbonate or similar host rocks (Bullen and Kendall, 1998). $\delta^{13}C$ is reported relative to the Vienna Pee Dee Belemnite (VPDB) standard. While the age of water cannot be discerned using $\delta^{13}C$, differences may be attributed to different

lengths of groundwater flow, the type of flow path, or interactions of water with the soil horizon (added carbon dioxide (CO_2) from microbes connotes lighter $\delta^{13}C$ values). The typical $\delta^{13}C$ signature for soils is -15‰ (Chowdhury et al., 2004). Evolved (heavier) $\delta^{13}C$ signatures are indicative of longer residences times as a result of increased carbonate aquifer matrix interactions.

Radiogenic isotopes are produced by the decay of radioactive nuclei. Radiogenic isotopes commonly used in water resource assessments include Carbon-14 (^{14}C) of DIC, tritium (^{3}H), and strontium-87/86 ($^{87}Sr/^{86}Sr$) of dissolved strontium. Due to its long half-life, ^{14}C is useful as an environmental tracer to determine the age of groundwater when it was taken out of contact with the atmosphere. This metric is useful for discerning groundwater flow directions, spring catchment areas (or source areas), and rates of recharge (Bullen and Kendall, 1998; Knierim et al., 2013; Bhandary et al., 2015). ^{3}H is a hydrogen isotope used to identify and date recent groundwater, namely to differentiate between groundwater recharged before, during, or after atmospheric nuclear activities in the 1950s (Clark and Fritz, 1997). Because $^{87}Sr/^{86}Sr$ has negligible fractionation during mineral-water interactions, it is used as an environmental tracer to trace strontium due to weathering from specific geologic settings and strontium-bearing minerals (Banner and Kaufman, 1994; Bullen and Kendall, 1998; Uliana et al., 2007).

Less common, but promising, isotopes with the potential to better understand complex recharge-discharge relations include boron-11 ($\delta^{11}B$), nitrogen-15 of nitrate ($\delta^{15}N\text{-}NO_3$), and oxygen-18 of nitrate ($\delta^{18}O\text{-}NO_3$). Boron is a conservative element, so the isotopic signature from its source area is preserved. Natural origins of boron concentrations and isotopic signatures in groundwater are derived from the leaching of rocks and soils in recharge areas and the aquifer matrix, as well as mixing with adjacent groundwaters (Davidson and Bassett, 1993; Nims, 1998; Kendall et al., 2005). $\delta^{11}B$ has also been demonstrated to be useful in anthropogenic contaminant source identification, particularly in water samples with detectable levels of boron (Vengosh et al., 1974; Pennisi et al., 2006; Foster et al., 2016). $\delta^{15}N\text{-}NO_3$ and $\delta^{18}O\text{-}NO_3$ can be useful in the identification of nitrate sources (Jung et al., 2020) and anthropogenic sources of contamination (Huebsch et al., 2014; Zhang et al., 2018; Veale et al., 2019), although the use of these isotopes in determining groundwater flow dynamics has challenges.

Geochemical assessments can be quite useful when characterizing complex recharge/discharge relations. Such assessments in water chemistry can highlight subtle differences in flow regimes and flow paths are not as easily discernable as through other methodologies, such as dye tracer tests and potentiometric surface mapping. Namely, the geochemical assemblage of a water sample can elucidate spatiotemporal variability in spring discharge, evolution along flow paths (e.g., water-host rock interactions), and sources of recharge that manifest as spring discharge.

Using ion concentrations and a multi-isotope approach can elucidate regional and local sources that contribute to a multi-outlet spring system.

Hydrogeologic framework

Generalized stratigraphic units that comprise minor and major aquifers in the study area are denoted in Figure 4. Minor aquifers in the study area include the Capitan Reef Aquifer, Rustler Aquifer, Igneous Aquifer, and West Texas Bolsons Aquifer (Figure 5). As described by Hiss (1980) and Sharp (1990), the Capitan Reef Complex is an ancient reef trend that formed the margins of the Delaware Basin approximately 250 million years ago. Permian age strata of the Delaware Basin comprise three aquifers: 1) the Wolfcampian and Leonardian shelf with fracture-dependent permeability, 2) the high-permeability Guadalupian shelf-margin, and 3) the low-permeability Guadalupian and Ochoan basin fill consisting of clastics and evaporites. The Apache Mountains are exposures of the shelf-margin in Culberson County. The Rustler Aquifer includes the Ochoan-age Rustler Formation. Dissolution of calcite, dolomite, gypsum, and halite and cation exchange dominate groundwater assemblages in the Rustler Formation (Boghici and Van Broekhoven, 2001). Tertiary-age igneous and volcaniclastics in the Davis Mountains are part of the Igneous Aquifer. The West Texas Bolsons Aquifer includes several deep basins of Quaternary sediments, including the Salt Basin. The Salt Basin graben is west of the Apache Mountains and resulted from basin and range faulting (Muehlburger and Dickerson, 1989). It includes the Wild Horse Flat sub-basin, which comprises thick, alluvial fan deposits that accumulated from the Precambrian mountains to the west. Clastic sediments, and likely gypsum and caliche, fill the Salt Basin by as much as 2,400 feet thickness (Gate et al., 1980).

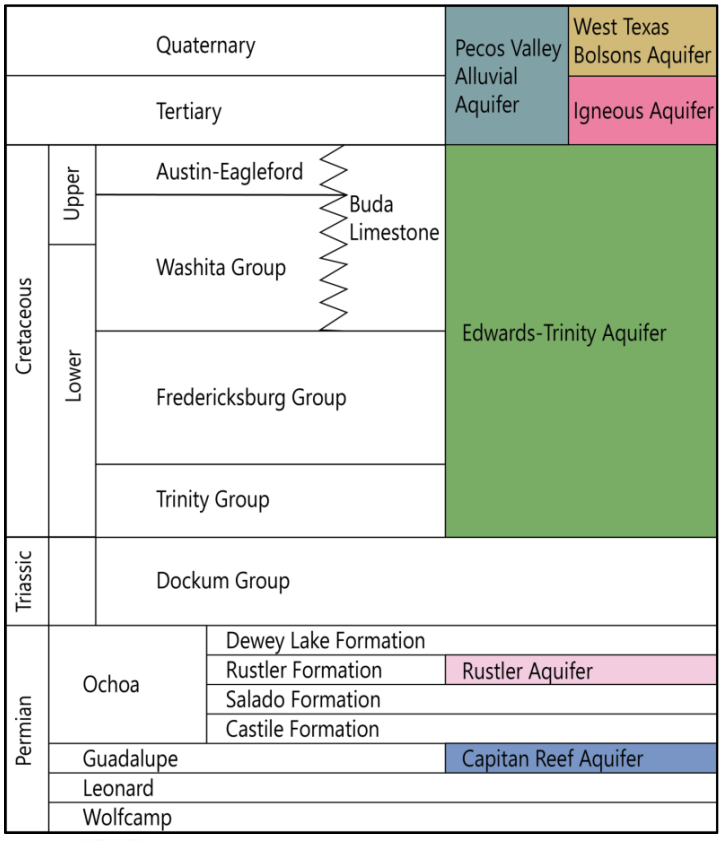

Figure 4. Generalized stratigraphy and associated major and minor aquifers in the study area (modified from Barker and Ardis, 1996).

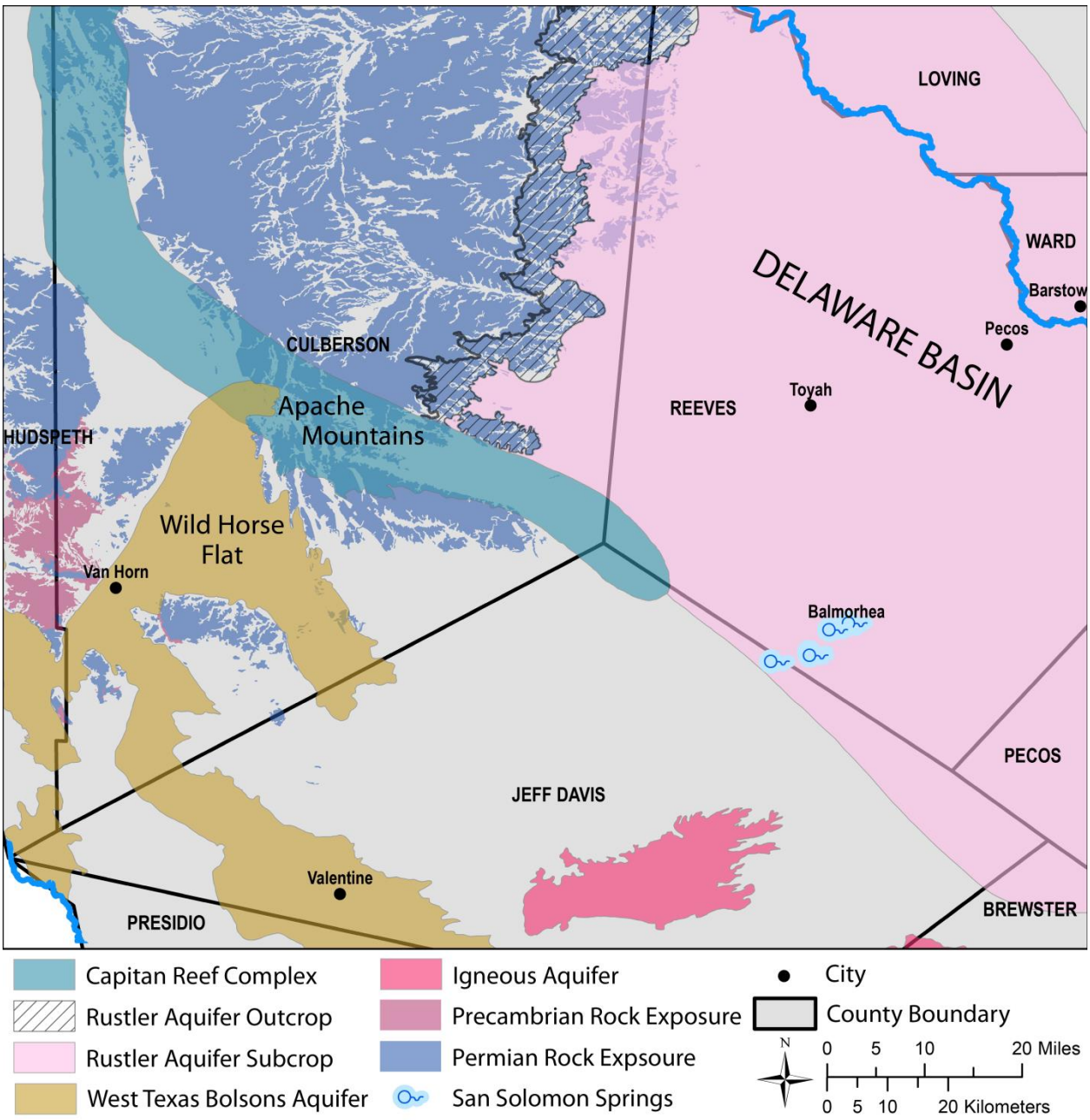

Figure 5. Minor aquifers in the study area.

Major aquifers in the study area include the Edwards-Trinity (Plateau) Aquifer (hereafter referred to as the Edwards-Trinity Aquifer) and the Pecos Valley Alluvial Aquifer (Figure 6). Upper Cretaceous rocks in the Edwards-Trinity Aquifer include limestone, marl, and clay in the Washita Group. Lower Cretaceous rocks consist of limestone in the Fredericksburg Group and sand, limestone, and shale in the underlying Trinity Group (Barker et al., 1994). Remnants of the Buda Limestone overly and are not part of the Edwards-Trinity Aquifer. The Pecos Valley Alluvial

Aquifer, referred to as the Cenozoic Pecos Alluvium when saturated and permeable, overlies the Cretaceous units and consists of Tertiary and Quaternary alluvial deposits (sands, gravels, silt, clay, and caliche) (LaFave and Sharp, 1987; Anaya and Jones, 2009).

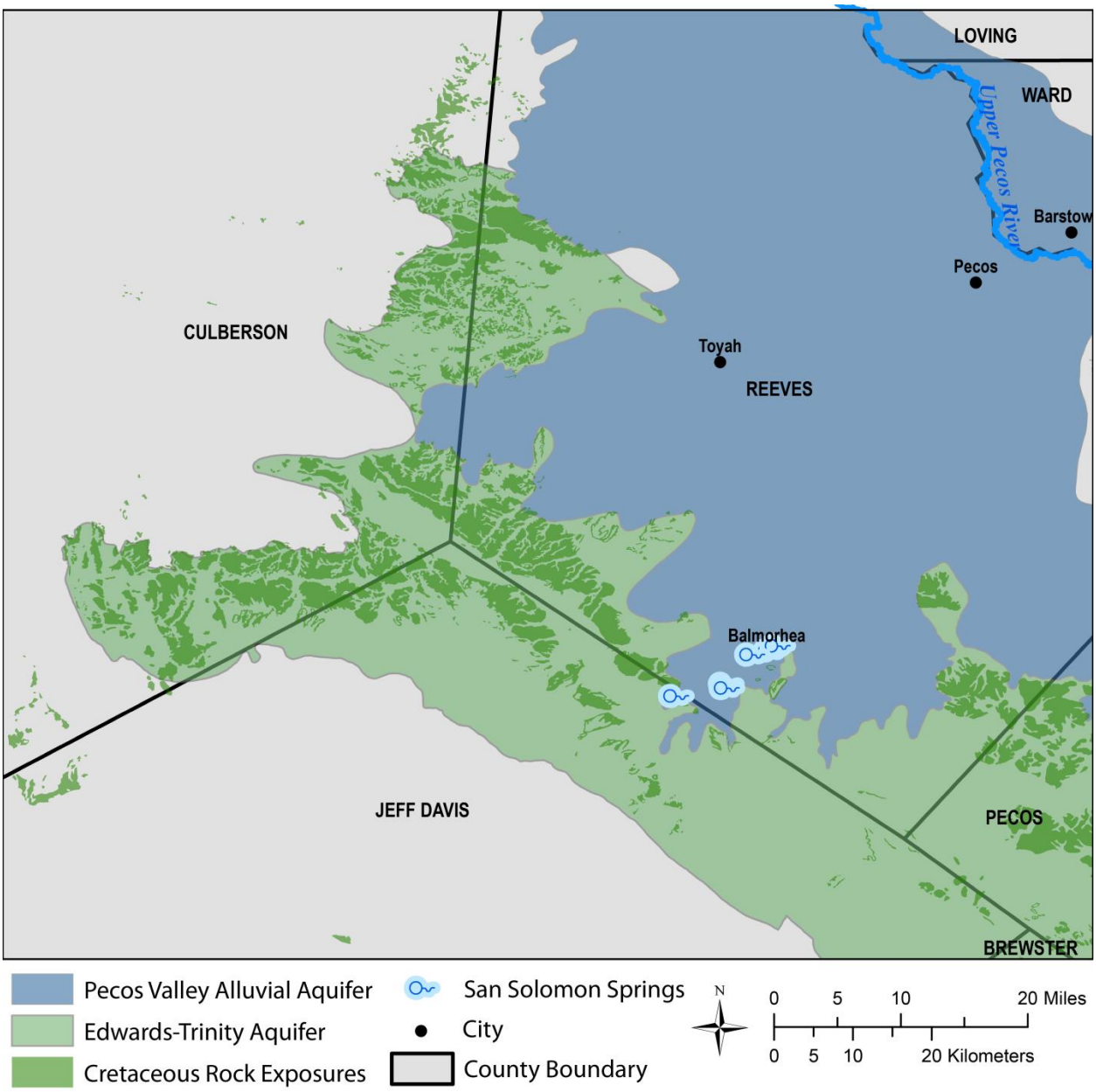

Figure 6. Major aquifers in the study area.

The exposed geologic units near Balmorhea and the springs include marine sediments of Cretaceous age, Tertiary volcanic rocks and lava flows in the Davis Mountains, and alluvial deposits of Quaternary age (White et al., 1941; Figure 7). Interconnected faults, fractures, and solution cavities characterize the Lower Cretaceous rocks, namely the Buda Limestone. The Cretaceous Buda Limestone overlies and is hydrologically continuous with the Washita Group, but it is not part of the Edwards-Trinity Aquifer (Barker et al., 1994). The Upper Cretaceous rocks are low permeability and mostly clay rich. High porosity lava flows in the Tertiary rocks that rest unconformably over Cretaceous rocks allow groundwater to enter the Lower Cretaceous units through seepage along the western limb of the Rounsaville Syncline (White et al., 1941). The Cenozoic Pecos Alluvium in the Toyah Basin is in hydraulic communication with underlying Cretaceous units in Reeves County (LaFave, 1987). The Toyah Basin was created by the dissolution of evaporite-salts of the Castile and Salado formations and gypsum from the Rustler Formation (Ashworth, 1990). Similar dissolution processes, normal faulting, and Tertiary volcanism also created the Rounsaville Syncline and the Stocks Fault (Figure 7). All of these rocks are underlain by Triassic, Permian, and older strata deposited northwest in the Delaware Mountains.

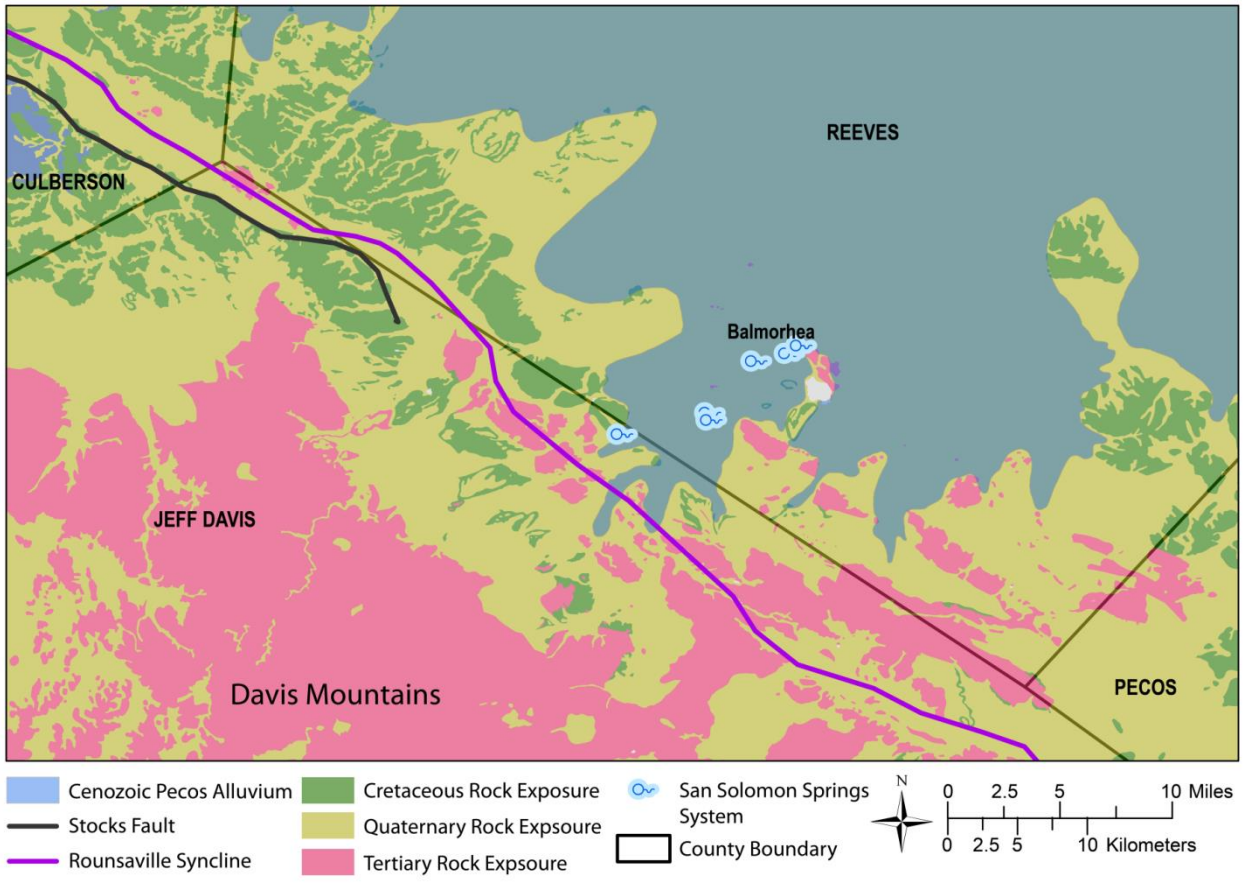

Figure 7. Exposed geologic units and aquifers near Balmorhea and San Solomon Springs.

Methods and approach

Data collection

Spring and well samples were collected to be analyzed for a robust suite of hydrochemical constituents. Field campaigns were conducted in February 2019, December 2019, and September-October 2020 to sample all six springs of San Solomon Springs. In December 2019, Upper Cretaceous, Cenozoic Pecos Alluvium, and Tertiary Volcanics aquifer wells were also sampled (Figure 8). Wells were purged for thirty minutes prior to sampling until hydrochemical parameters stabilized. Due to limited site access, Phantom Lake Spring was not sampled during the 2020 field campaign.

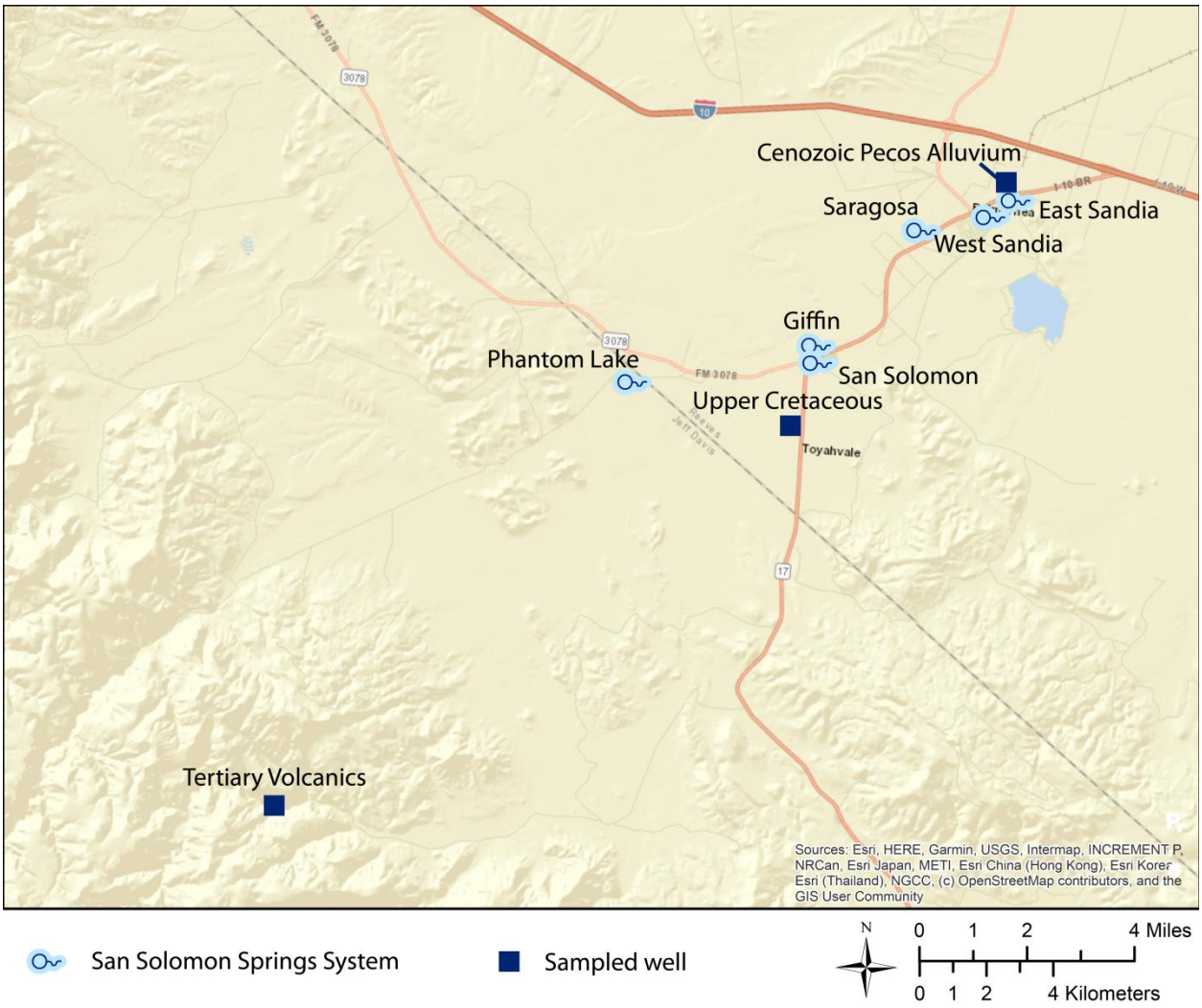

Figure 8. Spring and well sample locations.

In-situ measurements of specific conductivity, temperature, pH, and alkalinity were made at the time of water-sample collection. A multi-parameter probe (Hach HydroLab MS5 Multiparameter Mini Sonde or Aqua TROLL 600) was used to measure specific conductivity, temperature, and pH. The probe was calibrated each day using NIST-traceable standards. A three-point calibration was done at pH 4, 7, and 10. Specific conductivity was calibrated using a 1,413 µS/cm conductivity standard. Alkalinity samples were measured both in the field using an endpoint-titration method and by Lower Colorado River Authority Environmental Laboratory Services (LCRA-ELS).

All spring and groundwater samples were analyzed for dissolved ions, trace elements, SiO_2, and NO_3^-, which comprise the standard suite of analytes recommended by the Texas Water Development Board (TWDB) for groundwater samples (Boghici, 2003). Sample collection and preservation protocols and retention times for each hydrochemical constituent are described Table 1. Water samples were collected in pre-acidified and/or pre-cleaned high density polyethylene (HPDE) or amber glass sample bottles provided by LCRA-ELS.

Table 1. List of sample types, containers, and preservation methods.

Constituent	Container	Preservation	Retention Time
Major cations, trace metals	250 mL HDPE	Filtered, HNO_3 to pH<2, chilled to <4°C	6 months
Major anions; alkalinity	500 mL HDPE	Filtered, chilled to <4°C	28 days; 7 days
Nitrates	250 mL HDPE	H_2SO_4 to pH<2, chilled to <4°C	28 days
$\delta^{13}C$ and ^{14}C in water	1 L HDPE	chilled to <4°C	Send to lab within 30 days of collection
$\delta^{2}H$ and $\delta^{18}O$ in water	250 mL HDPE	chilled to <4°C	Send to lab within 30 days of collection
^{3}H in water	500 mL HDPE	chilled to <4°C	6 months
$^{87}Sr/^{86}Sr$ in water	250 mL HDPE	Filtered, HNO_3 to pH<2, chilled to <4°C	6 months
DIC	250 mL amber glass	chilled to <4°C	7 days
$\delta^{11}B$ in water	1 L amber HDPE	Unfiltered, stored at room temperature	Indefinite

Hydrochemical data from this study's field campaigns in 2019, along with historical data from TWDB's Groundwater Database (TWDB, 2019), and Texas Parks and Wildlife (TPWD) (TPWD, 2019) are used in the analyses. Analytical results from the 2020 field campaign were not received in time to be included in this analysis. This combined dataset includes 36 records of field parameter data (Appendix A), 55 records of ion chemistry (Appendix B), and 37 records of isotopic data (Appendix C) from the six springs and three wells. Ion concentrations are

converted from milligrams per liter (mg/L) to milliequivalents per liter (meq/L) to account for chemical equivalence using conversion factors provided by Hem (1985). Charge-balance error (CBE) is calculated for each record to judge the validity and quality of the analytical results (Equation 1). All 55 records of ion concentrations used in this study have CBEs within ±5%.

$$CBE = \frac{\sum \text{meq cations} - \sum \text{meq anions}}{\sum \text{meq cations} + \sum \text{meq anions}} \; x \; 100 \quad (1)$$

Laboratory analyses

LCRA-ELS used inductively coupled plasma (ICP)-optical emission spectroscopy to quantify major cations, ion chromatography for major anions, and ICP-mass spectroscopy (ICP-MS) for trace metals. Stable and radiogenic isotopic analyses were conducted by various independent laboratories. The Tritium Laboratory of the Rosenstiel School of Marine and Atmospheric Science, University of Miami analyzed for 3H by gas proportional counting of H_2-gas. Stable isotopes of water, $\delta^{18}O$ and $\delta^{2}H$, and dissolved inorganic carbon (DIC), $\delta^{13}C$, were analyzed by Beta Analytic, Inc. (Miami, FL) using cavity ring down spectroscopy (for water) or gas chromatography isotope ratio mass spectrometry (for DIC). Tetra Tech Boron Isotope Laboratory in Fort Collins, Colorado measured boron ($\delta^{11}B$) isotopic composition by negative thermal ionization mass spectrometry. Lastly, $^{87}Sr/^{86}Sr$ of dissolved Sr in water was analyzed at the MIT Isotope Laboratory, Massachusetts Institute of Technology using multi-collector thermal ionization mass spectroscopy (MC-TIMS).

Geochemical analyses

Numerous techniques are employed to visualize and interpret the geochemical data. The Geochemist's Workbench® 14 (GWB 14) software (Bethke, 2008; Bethke et al., 2020) is used to generate cross-plots, box plots, and trilinear diagrams to provide graphical comparisons of the samples. GWB 14 is also used to calculate speciation of dissolved elements and the saturation index (SI) of various minerals in solution (Equation 2),

$$SI = \log\left(\frac{IAP}{K_{sp}}\right) \quad (2)$$

where IAP is the ion activity product and Ksp is the solubility product constant for the mineral. SI is an index that indicates whether conditions in the solution are thermodynamically favorable for a mineral to either precipitate or dissolve (Hem, 1985). For a given solution composition, a mineral is oversaturated if SI > 0 and undersaturated if SI < 0. If SI = 0, the mineral is at thermodynamic equilibrium. Kinetics and other factors influence whether a mineral that is calculated to be oversaturated or undersaturated will actually precipitate or dissolve. Because of analytical uncertainties, equilibrium conditions are likely for SI values between −0.1 and 0.1.

Multivariate statistical analyses

In this study, principal component analysis (PCA) and exploratory factor analysis (EFA) are performed as dimensionality reduction techniques. PCA uses linear combinations of variables to simplify the data into a smaller number of components which account for most of the variability present in a dataset (Bro and Smilde, 2014). A sample correlation matrix of the data is used to compute eigenvalues and eigenvectors. Eigenvectors are the principal component directions and eigenvalues are the principal component magnitudes. EFA produces similar results as PCA but aims to identify underlying factors that explain the variance among a set of variables. In EFA, latent variables are unknown and not directly observed or measured but are identified to explain the original data. EFA finds one or more common factors that cause the responses of measured variables.

PCA and EFA can provide clues to groupings (e.g., score plot) using a smaller number of variables. This might enable simplified fingerprinting because disparate chemical elements are retained but combined into fewer variables. This can then be used in subsequent analyses to discriminate or "fingerprint" the reduced number of raw variables that have the most impact. It can also help to identify important geochemical indicators that may explain variability among the spring system.

In this study, PCA and EFA are applied on a matrix of 55 records of geochemical data (Appendix B), all of which have nine variables (Ca^{2+}, Mg^{2+}, Na^{+}, K^{+}, HCO_3^{-}, SO_4^{2-}, Cl^{-}, NO_3^{-}, SiO_2). The multivariate statistical analyses are performed using the statistics software package Minitab 19 (Minitab 19 Statistical Software, 2019). The ensuing correlation matrix is used in PCA because the concentrations between different ions vary greatly. In EFA, principal component analysis is used for data extraction and varimax rotation is used for data rotation. PCA and EFA require that each record or observation has an observation for all of the variables in the statistical analysis. If a record is missing even one variable, then the entire record is removed. As an example, Saragosa Spring has only two records which have values for all nine variables both of which were collected during this study. In December 2019, NO_3^{-} at Saragosa Spring measured below the NO_3^{-} method detection limit (MDL) of 0.088 mg/L. Due to the limited number of samples for Saragosa Spring, NO3- on December 6, 2019 is assumed to be one half of the MDL, or 0.044 mg/L, to allow this record to be included in the statistical analyses.

Results

Field parameters

Considerable differences are apparent among the springs *in-situ* measurements of field parameters. Temperature measurements of the artesian springs are between 22.7 and 25.8 degrees Celsius (°C). East Sandia and West Sandia Springs are between 18.9 and 21.9°C. Temperature measurements at the artesian springs and Upper Cretaceous well are consistently higher than the gravity springs and Cenozoic Pecos Alluvium and Tertiary Volcanics wells (Figure 9). Higher temperatures are interpreted to reflect contributions from a deeper regional source (White et al., 1941; LaFave and Sharp, 1987). In contrast, lower temperature measurements at the gravity springs are consistent with contributions that are shallower or are mixed with another local source that lowers the temperature. Saragosa Spring exhibits greater variability in temperature which may suggest variable sources of recharge.

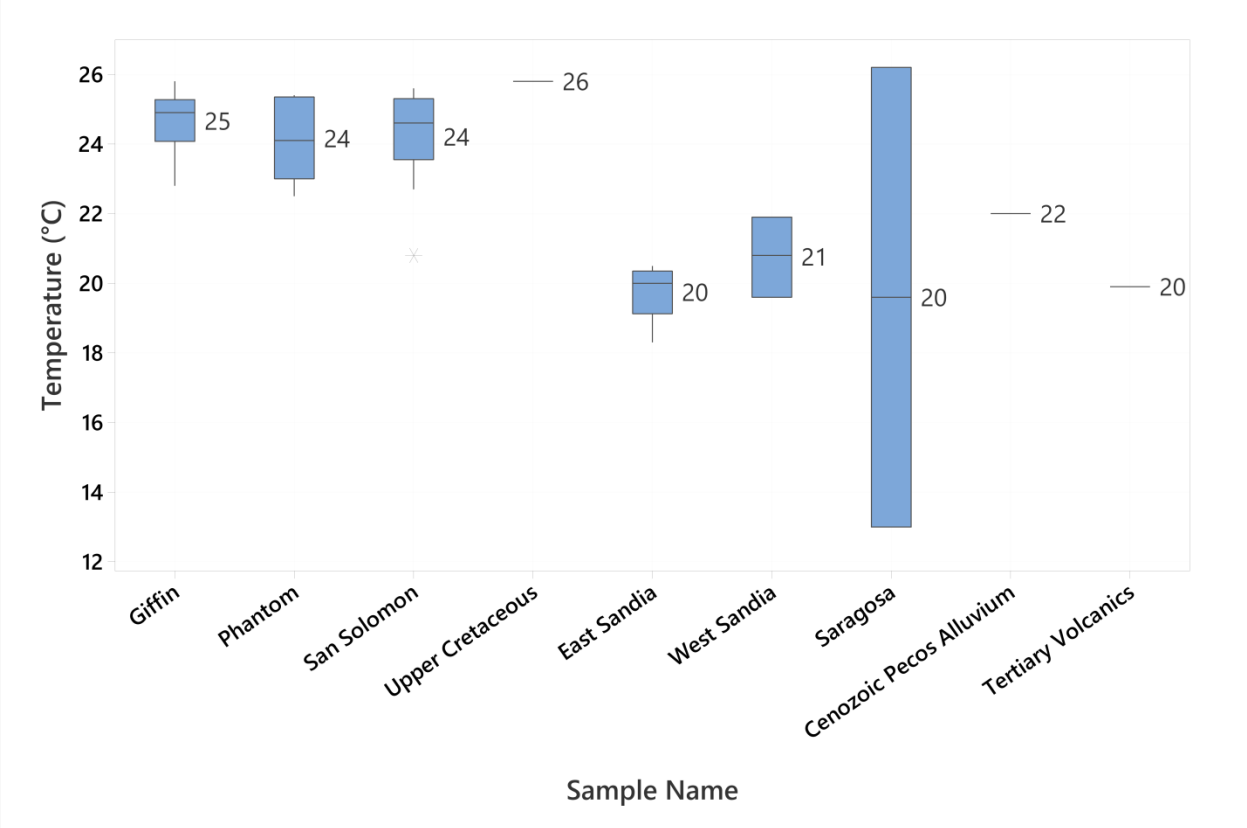

Figure 9. Interquartile ranges of temperature data for San Solomon Springs and surrounding wells. Mean temperatures are labeled on the right of each interquartile range.

Specific conductivity is the ability of an aqueous solution to carry an electrical current and correlates with dissolved ion concentrations (Hem, 1985). Specific conductivity measurements indicate differences exist between the springs and wells (Figure 10). The mean specific conductivity values for the artesian springs range from 2835 – 2950 microsiemens per centimeter (µS/cm). The Upper Cretaceous well and Saragosa Spring have mean specific conductivity measurements that are comparable to the artesian springs. Mean specific conductivity measurements for West Sandia Spring, East Sandia Spring, and the Cenozoic Pecos Alluvium well are also comparable and measure at 3757, 4123, and 3831 µS/cm, respectively.

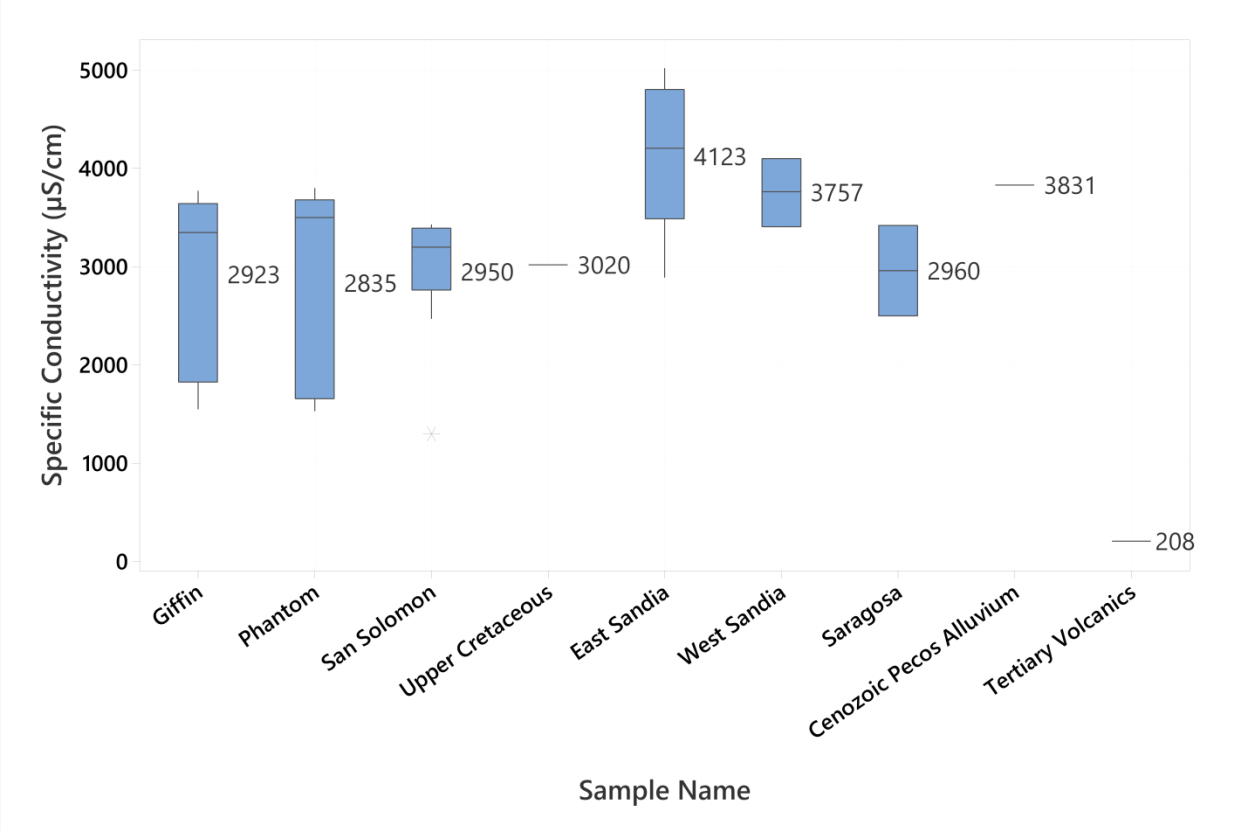

Figure 10. Interquartile ranges of specific conductivity data for San Solomon Springs and surrounding wells. Mean specific conductivity measurements are labeled on the right of each interquartile range.

Major ion composition

In general, the major ion data amongst the springs and surrounding wells exhibit similarities. As indicated in the Piper diagram (Piper, 1944), all six springs, the Upper Cretaceous well, and Cenozoic Pecos Alluvium well have dominant Na-Cl-SO_4 compositions (Figure 11). Saragosa Spring has one measurement that deviates from this cluster. The Tertiary Volcanics well has a markedly dissimilar hydrochemical facies compared to the rest of the samples. Figure 11 highlights the challenge of segregating the springs using classic methods due to this similarity of major ion composition.

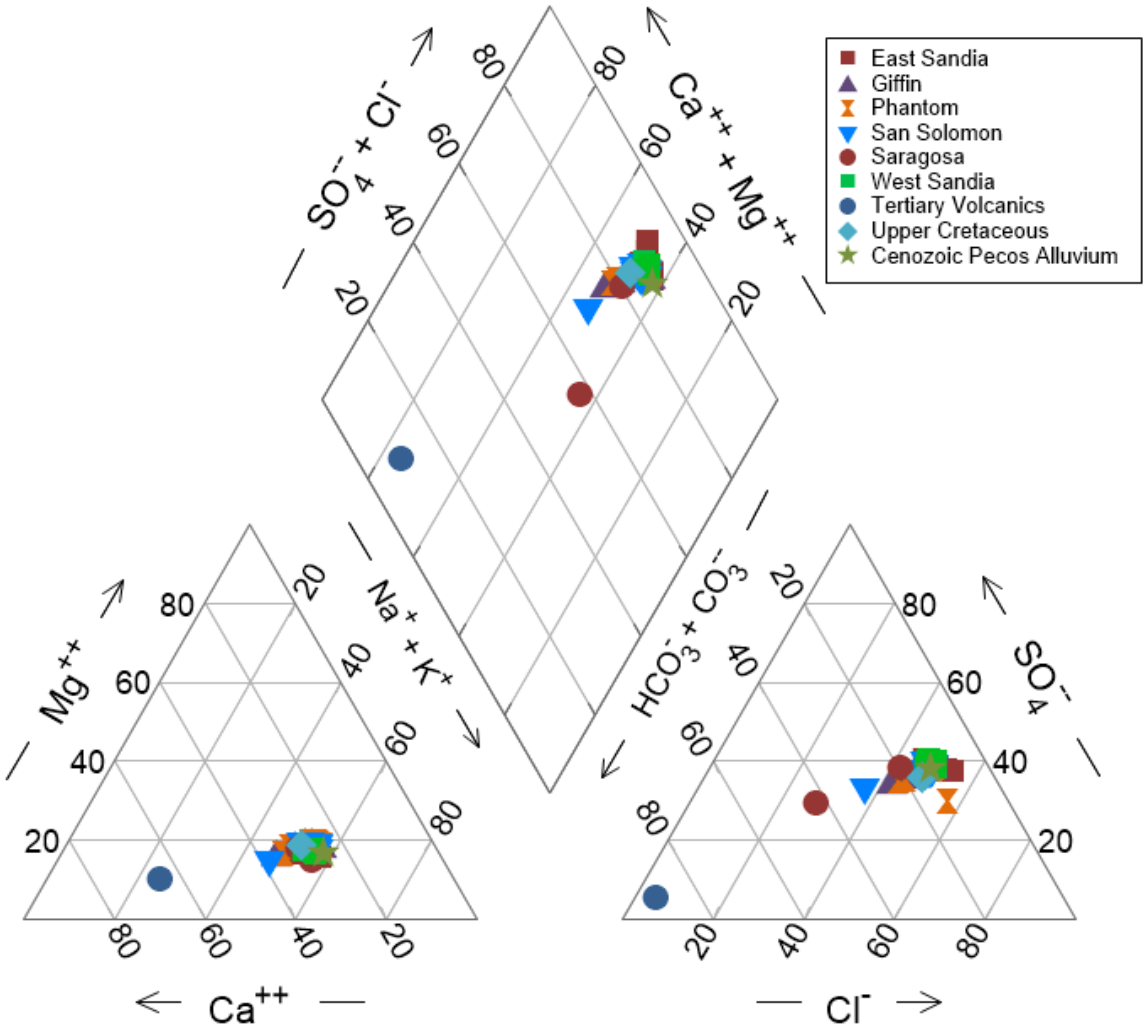

Figure 11. Piper diagram (in % meq/kg) showing sampled spring water from San Solomon Springs and surrounding wells.

A linear relationship for all spring and well samples is apparent in a cross-plot of Na^+ versus Cl^- (Figure 12). The source of Na^+ and Cl^- is likely derived from halite (NaCl). Excess Na^+ in almost all of the spring samples suggests there is an additional source of Na^+ to these waters. Spring groupings are apparent, with elevated stoichiometric ratios of Na^+ and Cl^- in West Sandia and East Sandia springs and the Cenozoic Pecos Alluvium well. A third spring grouping characterized by low Na^+ and Cl^- is also apparent in Phantom Lake, San Solomon, and Giffin spring samples. Two East Sandia Spring samples have approximately equal or elevated Cl^- with respect to Na^+.

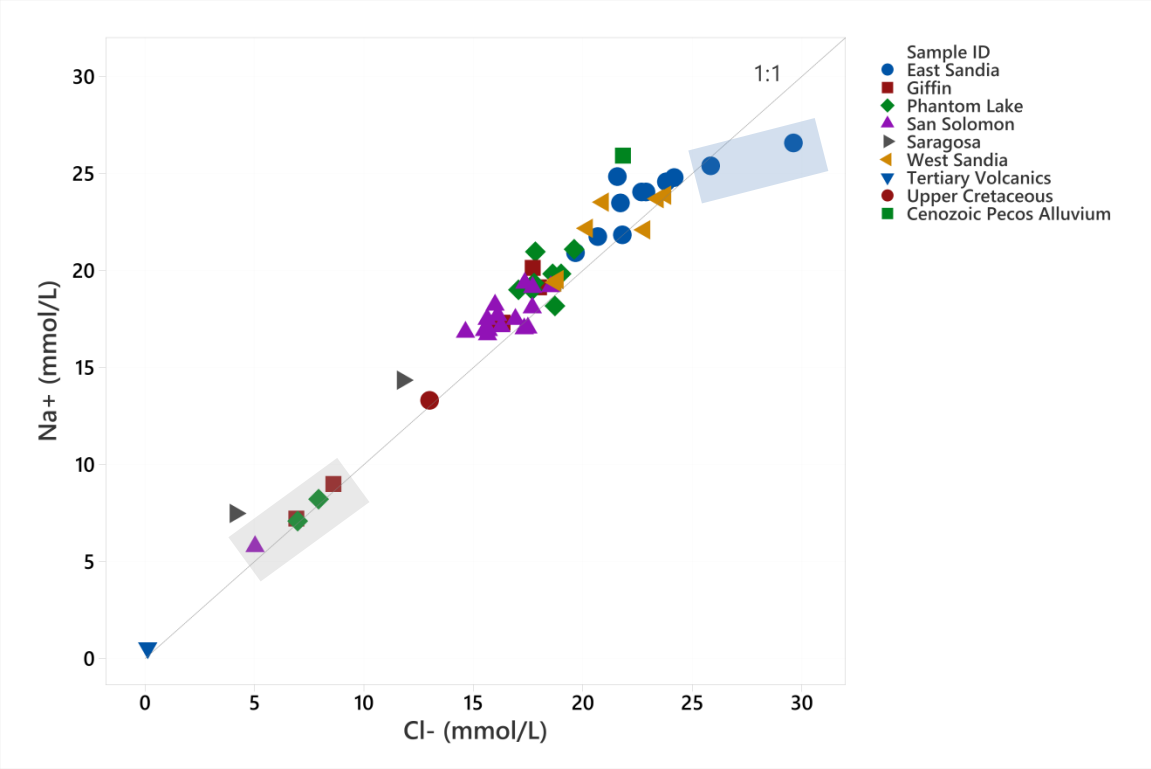

Figure 12. Relationship between Na^+ and Cl^- in mmol/L. The subset of artesian springs is outlined by the gray box. The two East Sandia Spring samples that deviate from the rest of the samples are outlined in blue.

Dissolution of calcite and dolomite are likely not the only sources of Ca^{2+}, Mg^{2+}, and HCO_3^- in San Solomon Springs and surrounding wells. Figure 13 illustrates the relationship between Ca^{2+} + Mg^{2+} with respect to HCO_3^-. Spring and wells samples would plot along the 1:2 reference line if these ions were strictly derived from carbonate rocks (i.e., calcite and dolomite). Groupings by spring type are evident, although the third subset of the artesian spring samples (gray box) and two East Sandia Spring records (blue box) plot separately. One Saragosa Spring sample and the Tertiary Volcanics well plot along this reference line.

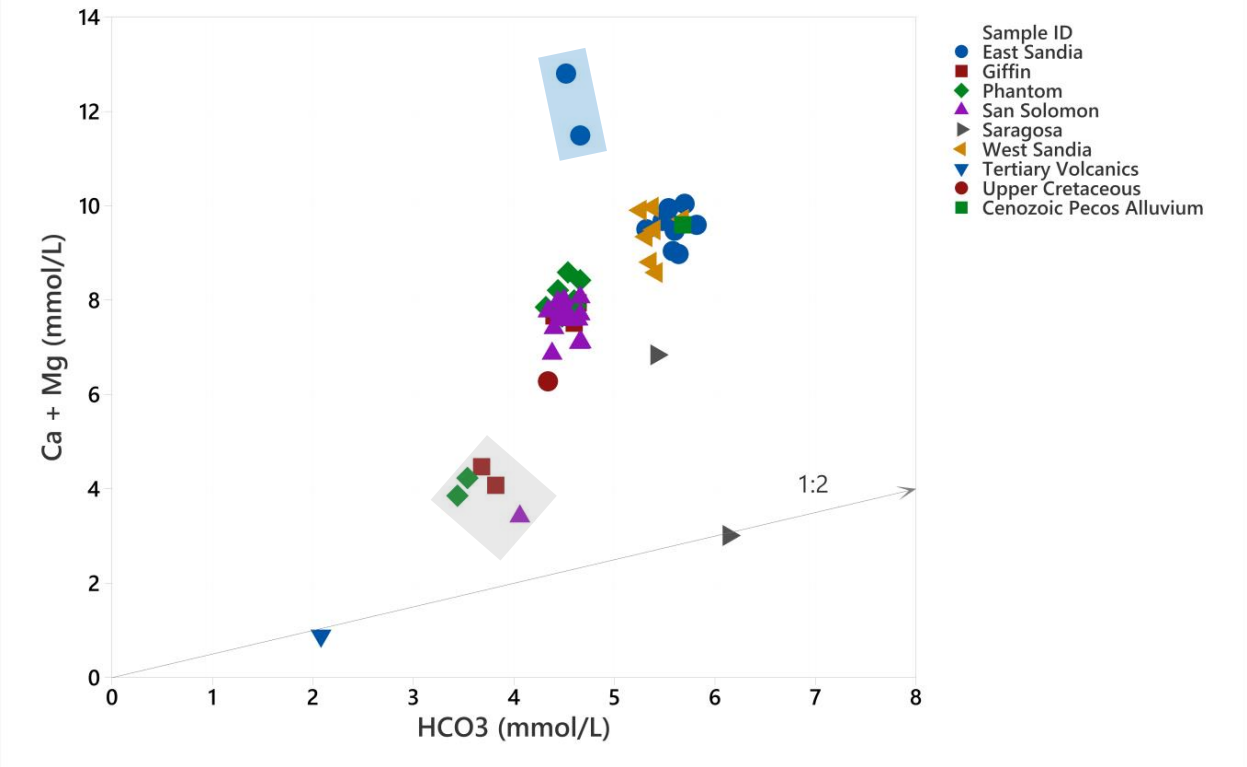

Figure 13. Cross-plot of Ca^{2+} + Mg^{2+} versus HCO_3^- in mmol/L. The subset of artesian springs is outlined by the gray box. The two East Sandia Spring samples that deviate from the rest of the samples are outlined in blue.

A cross-plot of Ca^{2+} plus Mg^{2+} minus HCO_3^- against SO_4^{2-} highlights excess SO_4^{2-} in almost all of the spring samples (Figure 14). Spring samples are grouped by spring type in this trend, and the subset of artesian springs and the two East Sandia samples are also apparent. Figure 14 indicates that the dissolution of anhydrite and gypsum accounts for SO_4^2 in these waters. The Sandia samples, in general, appear to have more loss of Ca^{2+} and Mg^{2+} compared to the rest of the samples. Thus, elevated Ca^{2+} and Mg^{2+} suggests additional gypsum and/or anhydrite dissolution occurs within the Cenozoic Pecos Alluvium.

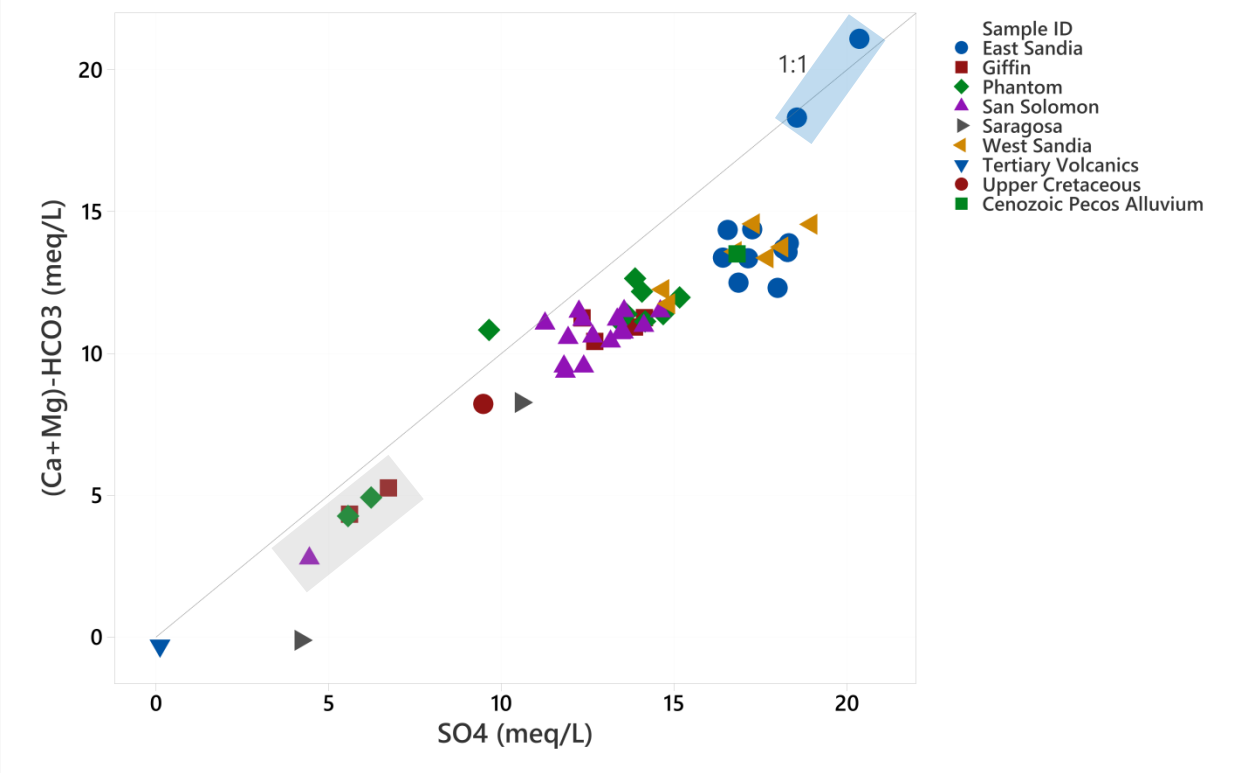

Figure 14. Cross-plot of (Ca^{2+} + Mg^{2+}) - HCO3- versus SO_4^{2-} in meq/L. The subset of artesian springs is outlined by the gray box. The two East Sandia Spring samples that deviate from the rest of the samples are outlined in blue.

Excess Na^+ (Figure 12) and the loss of Ca^{2+} and Mg^{2+} (Figure 14) suggest ion exchange may be occurring in this system. Ion exchange processes in San Solomon Springs and surrounding wells are evaluated in Figure 15. The 1:1 line is used to evaluate if ion exchange occurs (i.e., excess Na^+ replaces and accounts for the loss of Ca^{2+}+Mg^{2+}). The ellipse in Figure 15 illustrates most samples generally fall along the 1:1 line. However, a subset of samples outlined by the blue box deviates from this trend. These samples suggest there is excess Na^+ with respect to Ca^{2+}+Mg^{2+} unaccounted for by ion exchange.

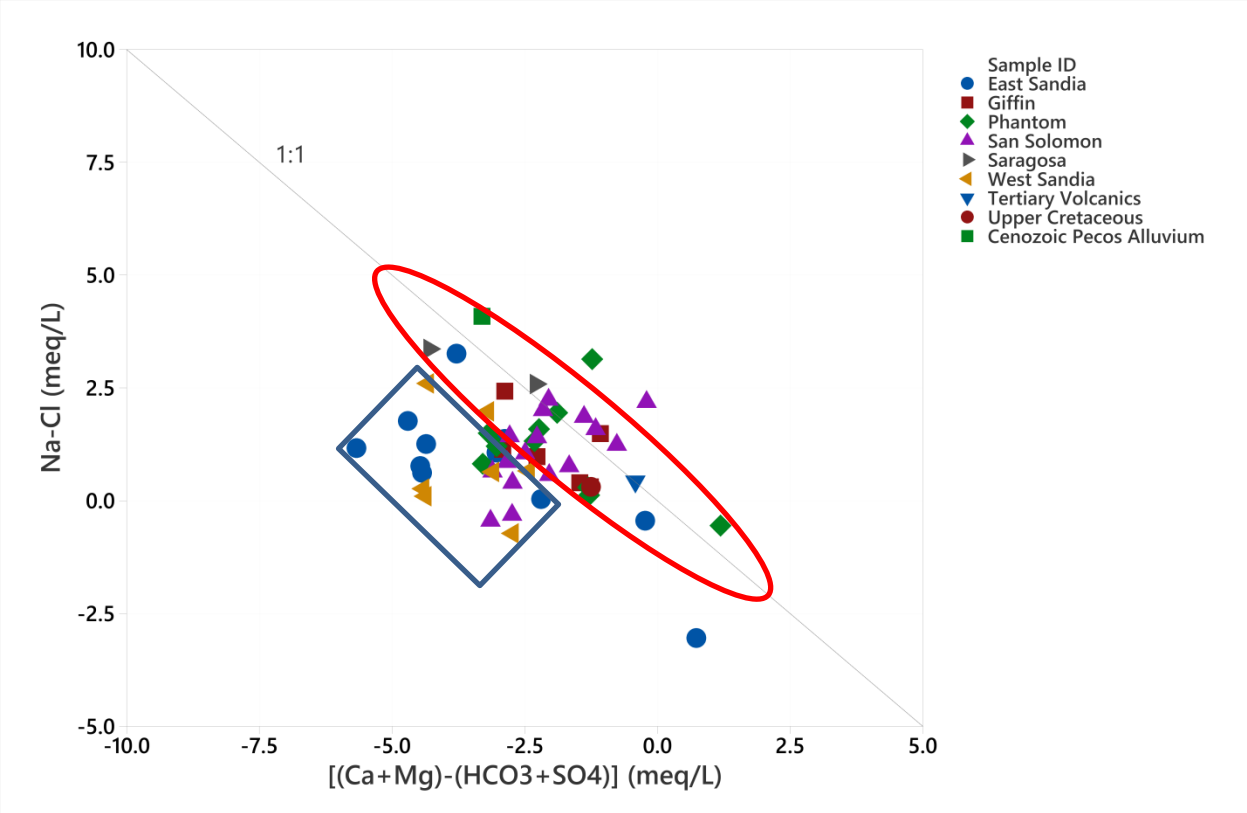

Figure 15. Cross-plot of (Na^+ - Cl^-) versus [(Ca^{2+} + Mg^{2+}) – (HCO_3^- + SO_4^{2-})] in meq/L.

San Solomon Springs has been documented to respond to rainfall events. This response is characterized by lower ion concentrations and by elevated turbidity and spring discharge. In late October/early November 1990, water was sampled from San Solomon, Phantom Lake, and Giffin springs four weeks after rainfall in the area (Robertson et al., 1990). Water chemistry data from these samples that are outlined by gray boxes plot separately from other samples of these springs in Figures 12-14. Samples from early August 2004 plot similarly with the 1990 samples. Because of the similarity of the 1990 and 2004 records, it is inferred that the 2004 records also represent hydrologic responses to rainfall. East Sandia Spring was also sampled during the 2004 campaign but did not exhibit reduced ion concentrations.

Boxplots of major ion concentrations without the low TDS samples from 1990 and 2004 for the artesian springs illustrate differences between San Solomon Springs and surrounding wells under inferred baseflow conditions (Figures 19-25). Samples from East Sandia and West Sandia springs measure consistently higher in Na^{+}, Cl^{-}, SO_4^{2+}, Ca^{2+}, HCO_3^{-}, SiO_2 (Figure 16), and NO_3^{-} (Figure 17) than the artesian springs and Saragosa Spring. With the exception of HCO_3^{-}, ion concentrations for Saragosa Spring appear to measure consistently at or below the artesian springs. The Tertiary Volcanics well exhibits markedly dissimilar chemistry than the rest of the samples, which is suggestive of a different hydrochemical facies as supported by the Piper Diagram (Figure 11).

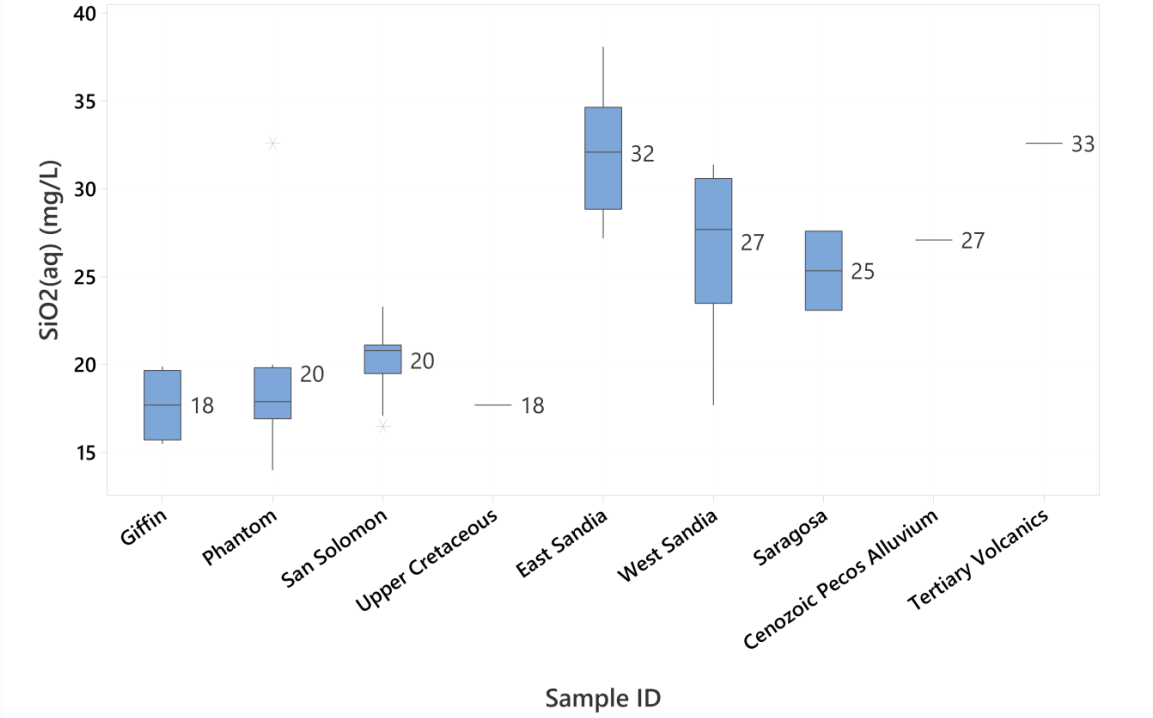

Figure 16. Interquartile ranges for baseflow SiO_2 concentration data for San Solomon Springs and surrounding wells. Mean SiO_2 concentrations are labeled on the right of each interquartile range.

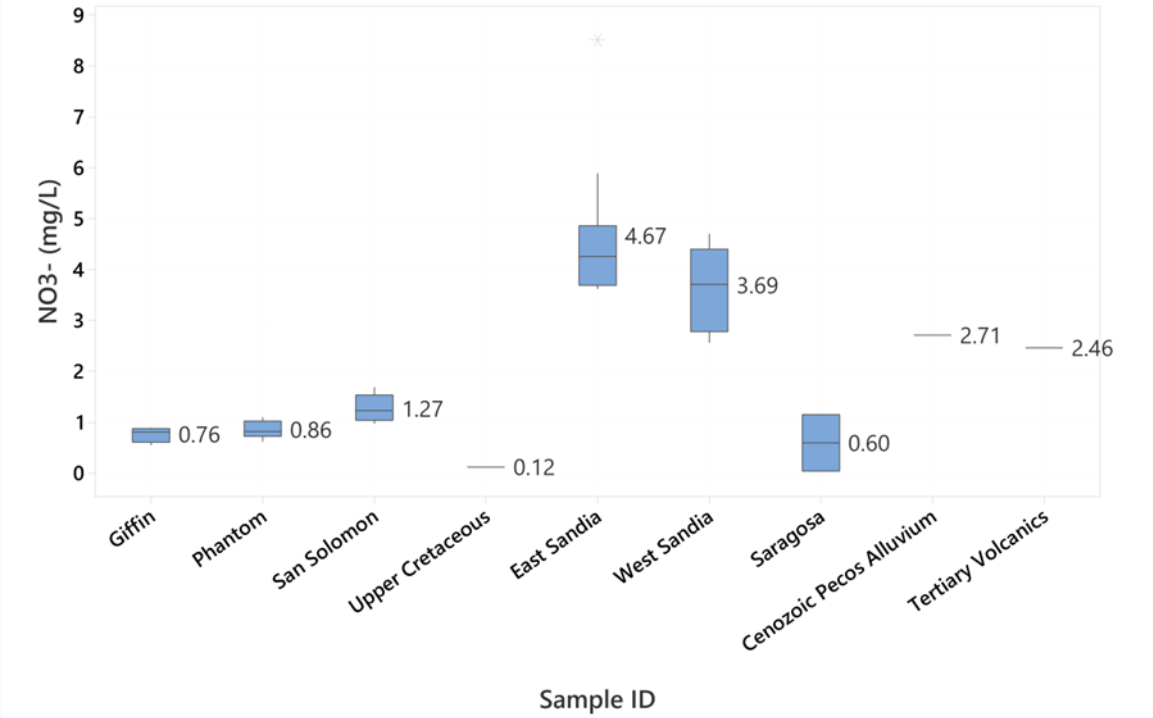

Figure 17. Interquartile ranges for all available NO_3^- concentration data for San Solomon Springs and surrounding wells. Mean NO_3^- concentrations are labeled on the right of each interquartile range.

Geochemical equilibria

The saturation states of water with respect to different mineral phases are outlined in Table 2Table 2. The springs are mostly at equilibrium with respect to calcite and dolomite and undersaturated with respect to amorphous silica, anhydrite, and gypsum. High pH values correlate with calcite saturation indices that approach 1, which may suggest pH values are impacted by CO_2 loss if measured far away from the spring outlet. Calcite and dolomite are mostly at equilibrium, which is consistent with the springs emanating from the carbonate system. Dedolomitization, the contribution of Mg^{2+} possibly from other rock types, and/or loss of Ca^{2+} via ion exchange may account for high SI values for dolomite.

Table 2. Saturation indices of various minerals calculated in GWB 14.

Sample ID	pH	Amorphous silica (log Q/K)	Anhydrite (log Q/K)	Calcite (log Q/K)	Dolomite (log Q/K)	Gypsum (log Q/K)
East Sandia	6.96	-0.52	-1.01	0.16	0.97	-0.77
East Sandia	6.81	-0.53	-1.01	-0.02	0.66	-0.78
Giffin	7.29	-0.83	-1.12	0.41	1.59	-0.94
Giffin	6.95	-0.87	-1.14	0.03	0.87	-0.96
Phantom Lake	7.04	-0.82	-1.08	0.15	1.11	-0.90
San Solomon	6.98	-0.78	-1.13	0.09	0.93	-0.93
San Solomon	6.91	-0.82	-1.14	-0.01	0.78	-0.96
Saragosa	7.38	-0.57	-1.27	0.39	1.42	-0.98
Saragosa	7.16	-0.48	-1.81	0.00	0.55	-1.51
West Sandia	7.06	-0.57	-1.06	0.23	1.15	-0.84
West Sandia	6.71	-0.58	-1.06	-0.12	0.48	-0.85
Tertiary Volcanics	7.21	-0.49	-3.41	-0.52	-0.97	-3.18
Upper Cretaceous	6.91	-0.81	-1.24	-0.03	0.69	-1.07
Cenozoic Pecos Alluvium	6.80	-0.59	-1.01	0.00	0.76	-0.80

Undersaturated conditions for amorphous silica, anhydrite, and gypsum may be expected given the relatively low TDS values for the springs and wells sampled. It is likely that waters from the springs and wells will dissolve these minerals. Low saturation indices for anhydrite and gypsum suggest waters are not in equilibrium with evaporites. It is possible that there are no large sources of evaporites contributing additional sulfates near the springs. Amorphous silica is also undersaturated which suggests waters are not in equilibrium with silicate minerals. East Sandia, West Sandia, Saragosa, and the Cenozoic Pecos Alluvium well have saturation indices for amorphous silica closer to 0 than Phantom Lake, San Solomon, Giffin, and the Upper Cretaceous well. There may be progress towards saturation for amorphous silica for East Sandia, West Sandia, and Saragosa springs as groundwater flows through the Cenozoic Pecos Alluvium to emanate at these springs.

Isotopes

Bumgarner et al. (2012) used annual weighted mean precipitation values for δ^2H and $\delta^{18}O$ from the nearest Global Network of Isotopes in Precipitation (GNIP) station in Chihuahua, Mexico (site 7622500) to represent stable isotopic signatures of precipitation in the study area. Representative values for the GNIP station for δ^2H and $\delta^{18}O$ are -44.0‰ and -6.50‰, respectively. Bumgarner et al. (2012) suggest that $\delta^{18}O$ greater than -7.50‰ represent waters reflective of local recharge conditions. Conversely, $\delta^{18}O$ less than -7.50‰ are indicative of older waters that reflect recharge during wetter and cooler conditions during the Pleistocene (Uliana et al., 2007).

A plot of δ^2H and $\delta^{18}O$ suggests that San Solomon Springs and surrounding wells are aligned with the GMWL (Craig, 1961; Figure 18). δ^2H and $\delta^{18}O$ values in Saragosa Spring and the Tertiary Volcanics well plot similarly and are enriched with respect to the rest of the springs and wells. Both Saragosa Spring and the Tertiary Volcanics well have $\delta^{18}O$ values greater than -7.50‰ which suggests a local climatic signal (i.e., recharge during the Holocene) is captured in these samples. With the exception of Saragosa Spring, San Solomon Springs have $\delta^{18}O$ values less than -7.50‰ (Appendix C), which indicates that older waters feed these springs. The Upper Cretaceous and Cenozoic Pecos Alluvium also have $\delta^{18}O$ values less than -7.50‰ and are interpreted to be recharged these older waters. Collectively, San Solomon, Phantom Lake, Giffin, West Sandia, and East Sandia springs are interpreted to be recharged by older waters from a cooler, Pleistocene climate.

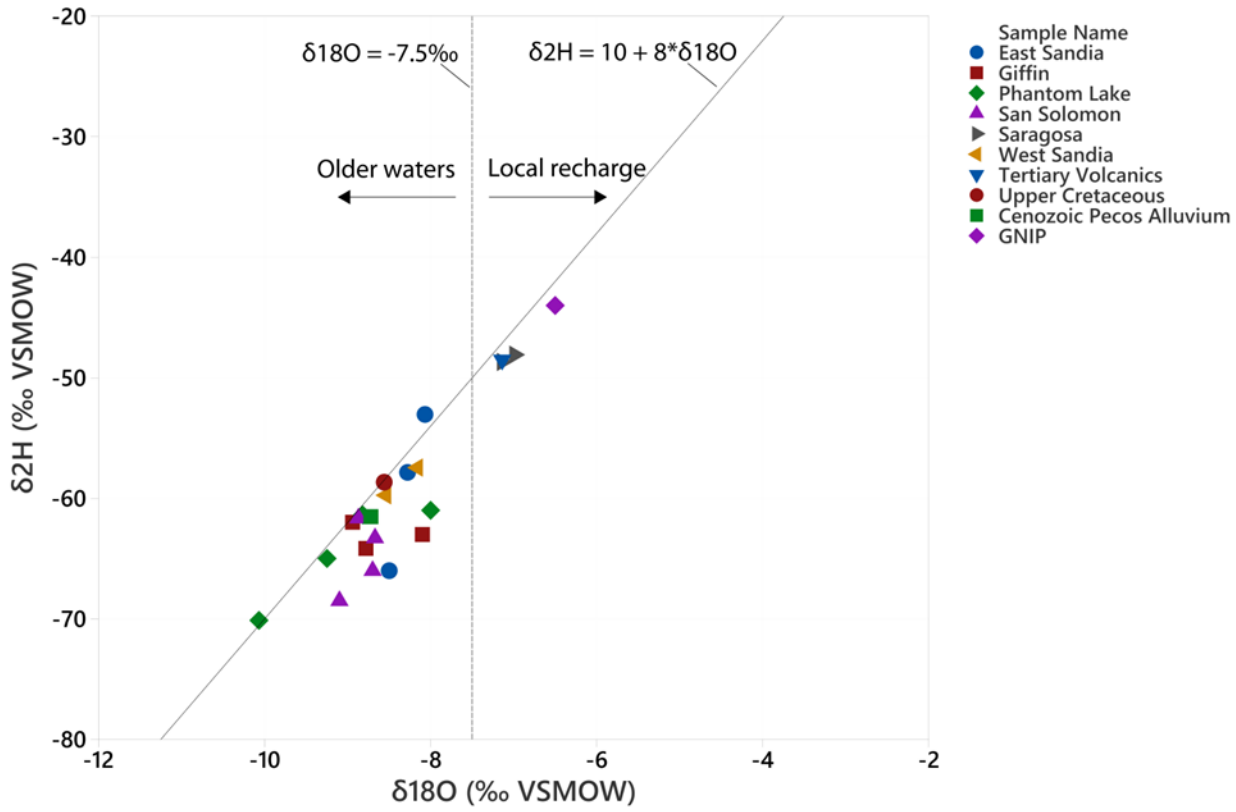

Figure 18. Relationship between δ^2H and $\delta^{18}O$ of San Solomon Springs and surrounding wells. Samples are plotted with respect to the GMWL and -7.5‰ $\delta^{18}O$ classification of older versus younger waters (Bumgarner et al., 2012; Uliana et al., 2007).

^3H is an isotope of hydrogen with a half-life of 12.43 years (IAEA, 1981). ^3H compositions in groundwater can be differentiated in waters that were produced relative to the 1950's atmospheric testing of nuclear bombs (Clark and Fritz, 1997). The classification of ^3H isotopic composition can be used to interpret the source of the water. For example, ^3H values less than 0.8 tritium units (TU) indicate waters are submodern and recharge occurred before 1950. ^3H values between 0.8 and 4.0 TU suggest mixing between submodern and recent recharge.

A plot of ^3H versus $\delta^{18}O$ suggests there are four different groupings of water with respect to ^3H and $\delta^{18}O$ classifications (Figure 19). San Solomon, Phantom Lake, Giffin, West Sandia, and East Sandia springs, the Upper Cretaceous well, and the Cenozoic Pecos Alluvium well fall into the pink cluster with ^3H and $\delta^{18}O$ values indicative of older recharge. Tritium is interpreted to be depleted at Phantom Lake and Giffin springs in this cluster. The Tertiary Volcanics well plots above the -7.5‰ $\delta^{18}O$ threshold but below 0.8 TU (blue cluster). This suggests waters were recharged during the Holocene but before the 1950's. In the green cluster, Phantom Lake and Giffin Spring in 2004, and San Solomon Spring in 2019 plot below -7.5‰ ($\delta^{18}O$) and above 0.8 TU. The oxygen isotopes retain the signal of older waters (i.e., from the Pleistocene) as a recharge source. However, a detectable level of ^3H above 0.8 TU in these samples suggests that

recharge to the artesian springs includes a mixing component with younger waters. Saragosa Spring is interpreted to have a modern source of recharge due to detectable levels of ^{3}H and heavy $\delta^{18}O$ signals (gray cluster).

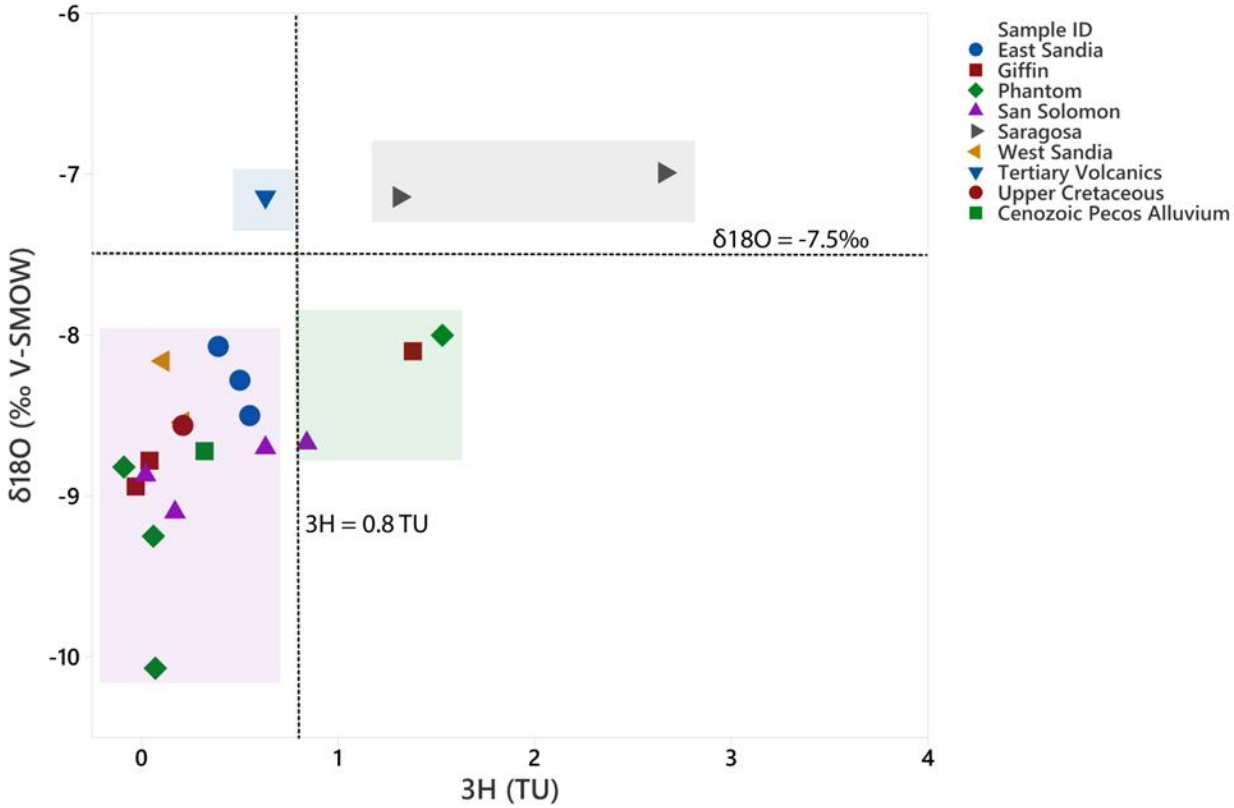

Figure 19. Relationship between $\delta^{18}O$ and ^{3}H of San Solomon Springs and surrounding wells. Samples are plotted with respect to the 0.8 TU classification of pre-1950's recharge (Clark et al., 1997) and -7.5‰ $\delta^{18}O$ classification of older versus younger waters (Bumgarner et al., 2012; Uliana et al., 2007).

$\delta^{13}C$ and percent modern carbon (pmC) can be used as an indicator of relative water-rock interaction. ^{14}C is produced in the atmosphere by cosmic ray interactions (Cook, 2020). Elevated modern carbon signatures signify more recent interactions with the atmosphere. Groundwater loses ^{14}C once it is taken out of atmospheric contact and as it interacts with the carbonate matrix over a transport pathway. $\delta^{13}C$ becomes larger as ^{14}C and pmC decrease. Less pmC can be interpreted to indicate that the water had more time to interact with carbonates—thus suggesting, longer or slower flow paths.

There are noticeable differences in $\delta^{13}C$ between the artesian and gravity springs. Values of $\delta^{13}C$ in samples from Phantom Lake, San Solomon, and Giffin Springs are between -7.40‰ and -6.00‰ under perceived baseflow conditions. These values of $\delta^{13}C$ at artesian springs are enriched with respect to the gravity springs, which are between -13.4‰ and -8.9‰ (Appendix

B). Smaller $\delta^{13}C$ values for East Sandia (-12.3‰), Giffin (-10.7‰), Phantom Lake (-11.4‰), and San Solomon (-9.86‰) springs were collected in August 2004.

A decrease in ^{14}C is interpreted to indicate that mostly all of the spring and well samples are part of the main flow system (Figure 20). Evolved pmC signatures for Giffin (0.10), Phantom Lake (0.09 – 0.11), and San Solomon (0.15) springs correspond to larger $\delta^{13}C$ that approach -6.0‰. Elevated pmC signatures for Giffin (0.38), Phantom Lake (0.39), and San Solomon (0.24) springs were collected in August 2004 and have smaller $\delta^{13}C$ values. $\delta^{13}C$ values for West Sandia (-9.1‰) and East Sandia (-8.9‰) springs and the Cenozoic Pecos Alluvium well (-8.7‰) and corresponding pmC signatures are outlined in gray in Figure 20. The modern carbon signatures (0.68, 0.74, 0.64, respectively) for these samples have more evolved (i.e., heavier) $\delta^{13}C$ values than one would expect over the deep carbonate transport pathway from the west. Saragosa Spring has a modern pmC signature of 0.94 that approaches $\delta^{13}C$ isotopic compositions representative of soils (-15‰) (Chowdhury et al., 2004).

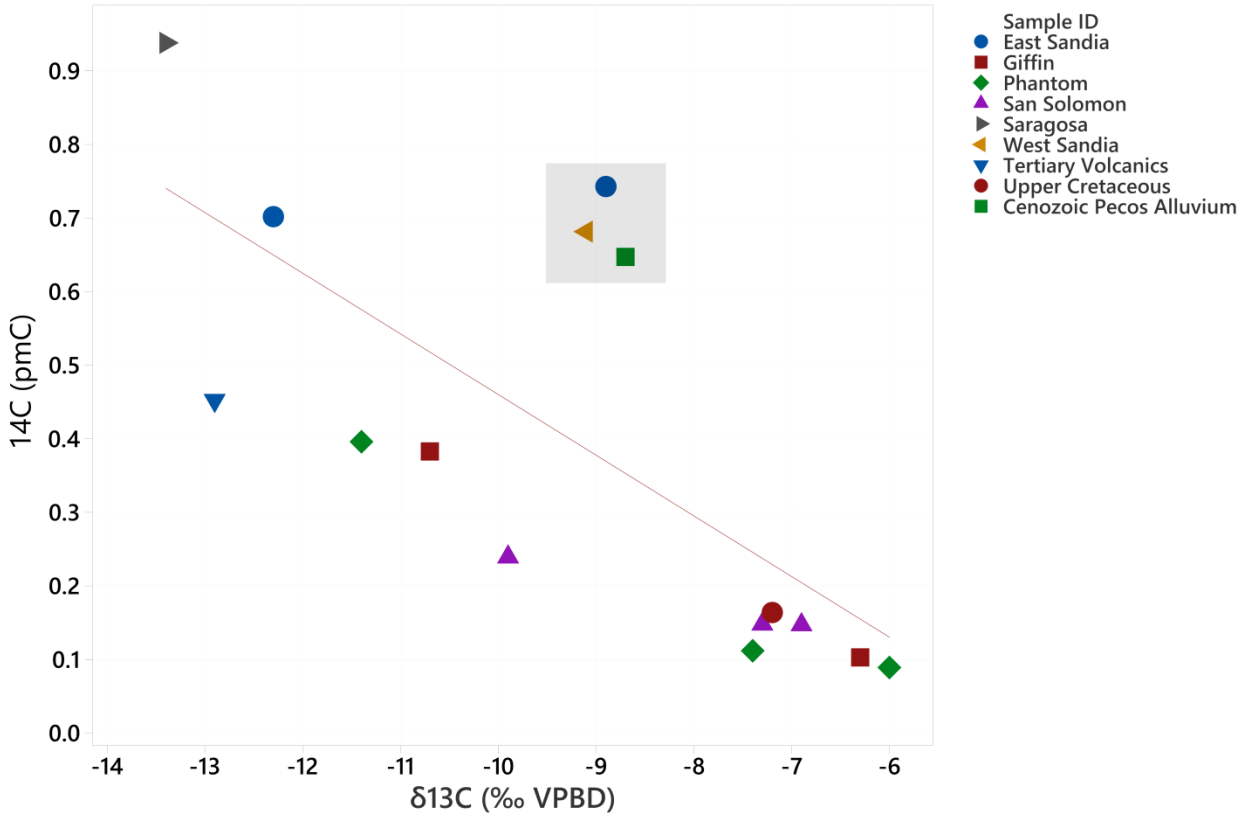

Figure 20. Relationship between ^{14}C and $\delta^{13}C$ of San Solomon Springs and surrounding wells. The gray cluster indicates elevated modern carbon signatures with respect to δ13C.

There is a general linear relationship between ^{3}H and ^{14}C, as ^{3}H content decreases as pmC decreases (Figure 21). Mixing lines are apparent. Most samples from the artesian springs have

low ^{14}C and low or non-detectable ^{3}H. The green mixing line with added ^{3}H and ^{14}C may represent dilution of Cretaceous water by precipitation. Low detectable levels of ^{3}H are unexpected for ^{14}C results that are less than 100 pmC. This suggests that mixing of older and younger water is captured in these measurements. East Sandia Spring, West Sandia Spring, and the Cenozoic Pecos Alluvium are on a different mixing line (blue line). There is much less ^{3}H but more ^{14}C. This mixing line may represent infiltration into the alluvium.

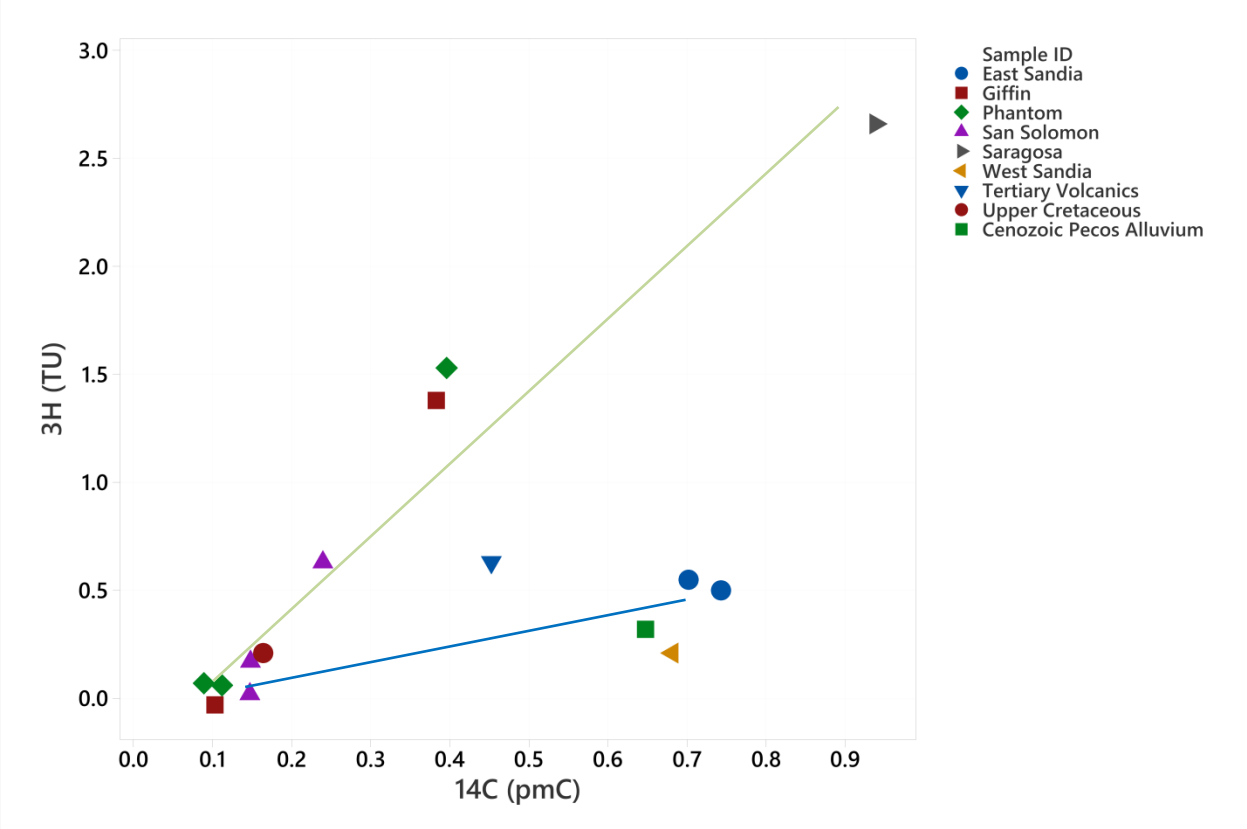

Figure 21. Relationship between pmC and ^{3}H of San Solomon Springs and surrounding wells.

$^{87}Sr/^{86}Sr$ ranges from 0.7030-0.7080 in samples from the Davis Mountains but can be as high as 0.728 (Burke et al., 1982; Cameron et al., 1996; Uliana et al., 2007). In the Permian and Cretaceous-age carbonates and evaporite waters, $^{87}Sr/^{86}Sr$ ranges from 0.7068 – 0.7084 (Burke et al., 1982; Brookins, 1988; Denison et al., 1998). Strontium isotopic compositions from the Precambrian and early Paleozoic silicate minerals in Wild Horse Flat and surrounding areas in the upgradient portions of the flow system are not documented in the literature (Uliana et al., 2007). Regardless, $^{87}Sr/^{86}Sr$ values from these rocks (i.e., siliciclastic and igneous rocks) are expected to be significantly higher than strontium isotope signatures from the Davis Mountains and Permian and Cretaceous-age carbonates and evaporites (Uliana et al., 2007).

$^{87}Sr/^{86}Sr$ signals in samples from all six springs are enriched in $^{87}Sr/^{86}Sr$ with respect to groundwater from the Davis Mountains and from the Permian and Cretaceous-age carbonates and evaporites (Figure 22). However, these elevated $^{87}Sr/^{86}Sr$ signals align with expected values from Wild Horse Flat. The Tertiary Volcanics well falls in line with expected values from the Davis Mountains. This suggests that the $^{87}Sr/^{86}Sr$ signal in all of the springs and wells is likely not conveyed by waters from the Davis Mountains.

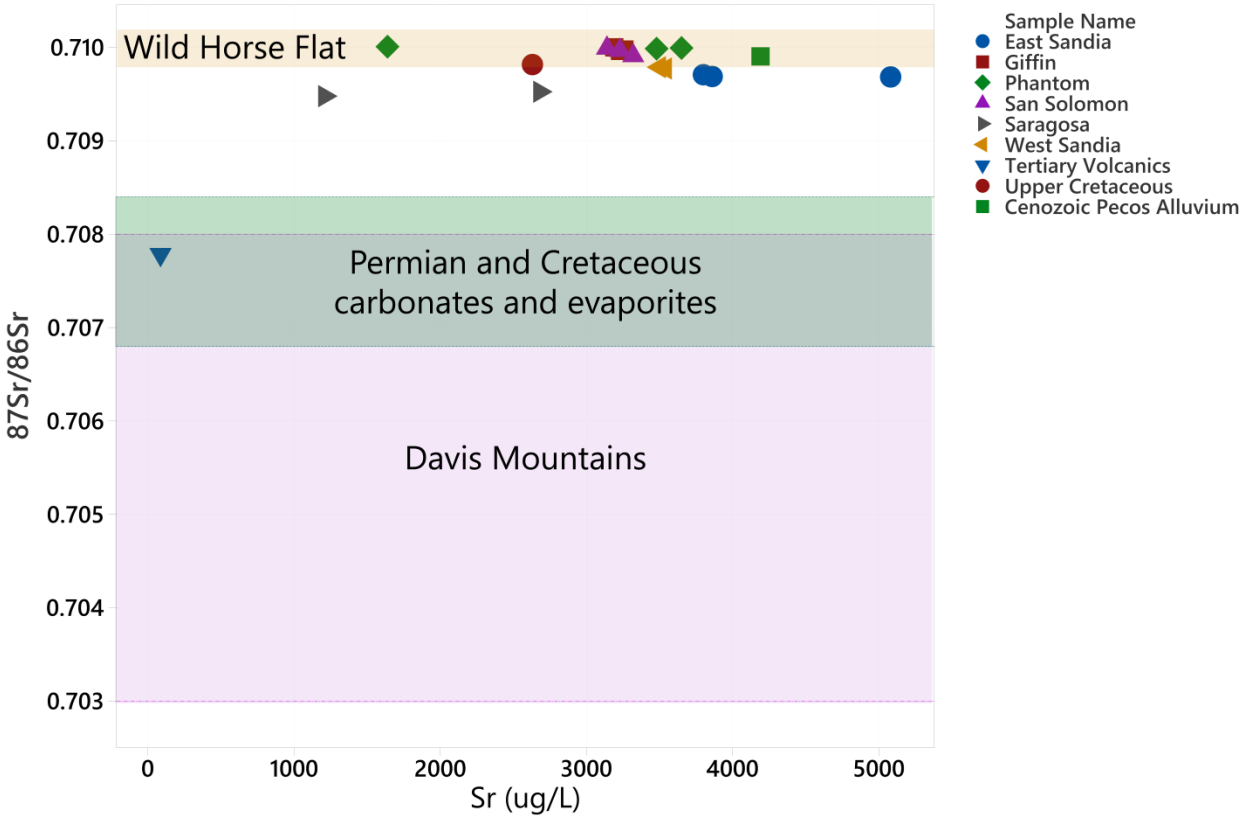

Figure 22. $^{87}Sr/^{86}Sr$ differentiation for surrounding geologic settings, San Solomon Springs, and the Upper Cretaceous, Tertiary Volcanics, and Cenozoic Pecos Alluvium wells.

Three distinct groupings of $^{87}Sr/^{86}Sr$ signals in waters from the springs of San Solomon Springs and surrounding wells samples are illustrated in Figure 23. Larger $^{87}Sr/^{86}Sr$ isotopic ratios in the green cluster include the artesian springs and the Cenozoic Pecos Alluvium well. East Sandia and West Sandia springs and the Upper Cretaceous well group together in a separate cluster (orange). Saragosa Spring has the lowest $^{87}Sr/^{86}Sr$ signals and Sr concentrations and groups separately (gray cluster). Moreover, the $^{87}Sr/^{86}Sr$ value for the Tertiary Volcanics well is 0.707782 and not plotted with the springs and wells in Figure 23.

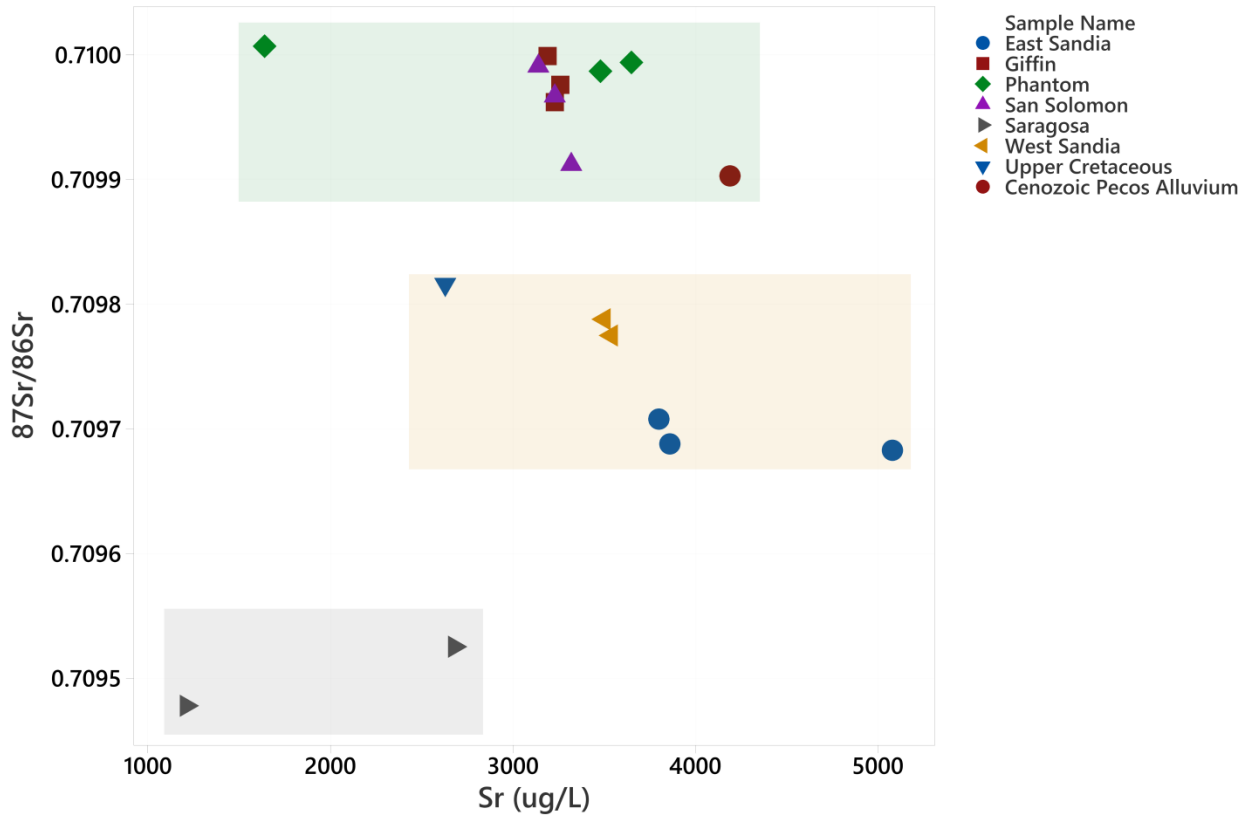

Figure 23. $^{87}Sr/^{86}Sr$ differentiation for San Solomon Springs and Upper Cretaceous and Cenozoic Pecos Alluvium wells.

Boron concentrations range from 143 to 680 µg/L in the artesian springs and 171 to 460 µg/L in the gravity springs (Appendix B). Isotopically distinct $\delta^{11}B$ signatures between the springs and wells, which range from 8.0 – 17.8‰, are not apparent. Moreover, potential anthropogenic impacts as indicated by $\delta^{11}B$ are not identified at this time. However, the inverse relationship between the inverse of dissolved boron (1/B) and $\delta^{11}B$ suggests that dissolved boron gradually increases as $\delta^{11}B$ increases (Figure 24), which may indicate natural origins of $\delta^{11}B$ in the springs and surrounding wells. The two separate mixing lines may be indicative of different origins of boron and $\delta^{11}B$ in this system. One mixing line has the Cenozoic Pecos Alluvium and San Solomon Spring as end members. East Sandia, West Sandia, and Giffin springs plot along this mixing line. Other samples from Saragosa Spring, Phantom Lake Spring, and the Upper Cretaceous well plot separately and may highlight a separate mixing line between the Cretaceous units and Phantom Lake and Saragosa springs.

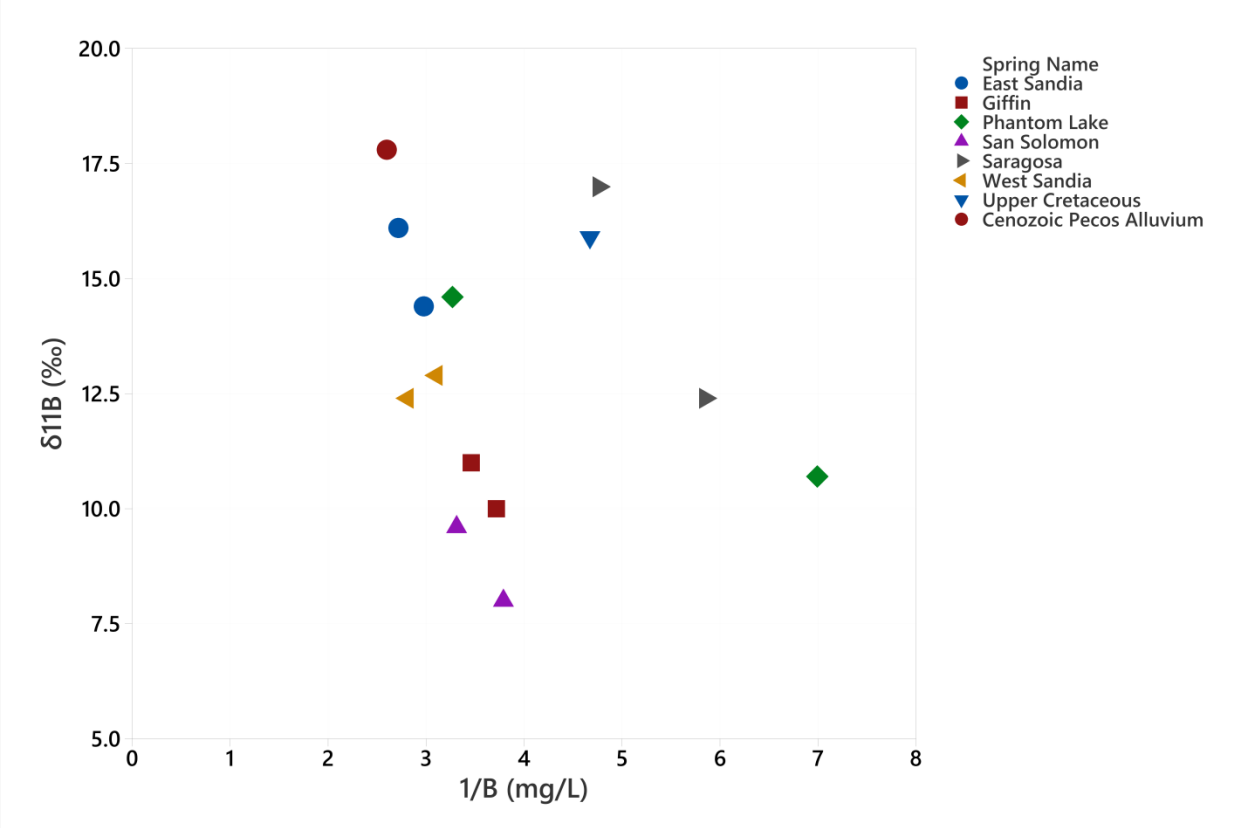

Figure 24. $\delta^{11}B$ differentiation for the San Solomon Springs System and Upper Cretaceous and Cenozoic Pecos Alluvium wells.

Multivariate statistical analyses

PCA indicates the first two principal components account for 89.0% of variability in the data. There are large positive associations with Ca^{2+}, Mg^{2+}, Na^{+}, K^{+}, Cl^{-}, and SO_4^{2-} in the first principal component (Table 3). The first component (PC1) accounts for 69.0% of the variability in the data. All of these variables contribute approximately equally to the first component, which emphasizes the difficulty of separating chemistries between all six springs. The second principal component (PC2) has large positive associations with NO_3^{-} and SiO_2 and accounts for an additional 20.1% of the variability in the data.

Table 3. Eigenvectors of the PCA.

	Variance (%)	Ca^{2+}	Mg^{2+}	Na^{+}	K^{+}	Cl^{-}	HCO_3^{-}	SO_4^{2-}	NO_3^{-}	SiO_2
PC1	69.0	0.385	0.382	0.397	0.387	0.392	0.296	0.395	-0.019	0.035
PC2	20.1	0.138	-0.159	-0.023	-0.073	0.032	0.03	0.032	0.687	0.689

When the PCA scores are calculated, one sees an effective separation that helps to identify different characteristics of the springs (Figure 25). The scores indicate phenomena represented in each component. For example, loadings for major ions in the first component are positive. Positive scores for this component indicate these samples have higher concentrations for these variables since the loadings are also positive. The artesian springs have essentially negative scores with respect to the first and second components, whereas the gravity springs have mostly positive scores. In other words, the gravity springs are elevated in Ca^{2+}, Mg^{2+}, Na^{+}, K^{+}, SO_4^{2-}, and Cl- in loading 1 and NO_3^{-} and SiO_2 in loading 2 (i.e., upper right quadrant). Conversely, the ion concentrations in the artesian spring waters are lower since the scores for these samples are mostly negative relative to both loading 1 and 2 (i.e., lower left quadrant). A third cluster has largely negative scores for loading 1 and positive scores for loading 2 (i.e., the upper left quadrant), so these samples have lower values for Ca^{2+}, Mg^{2+}, Na^{+}, K^{+}, SO_4^{2-}, and Cl- and higher values for NO_3^{-} and SiO_2. Saragosa Spring, two East Sandia Spring records, and the Upper Cretaceous well are somewhat outliers to this categorization.

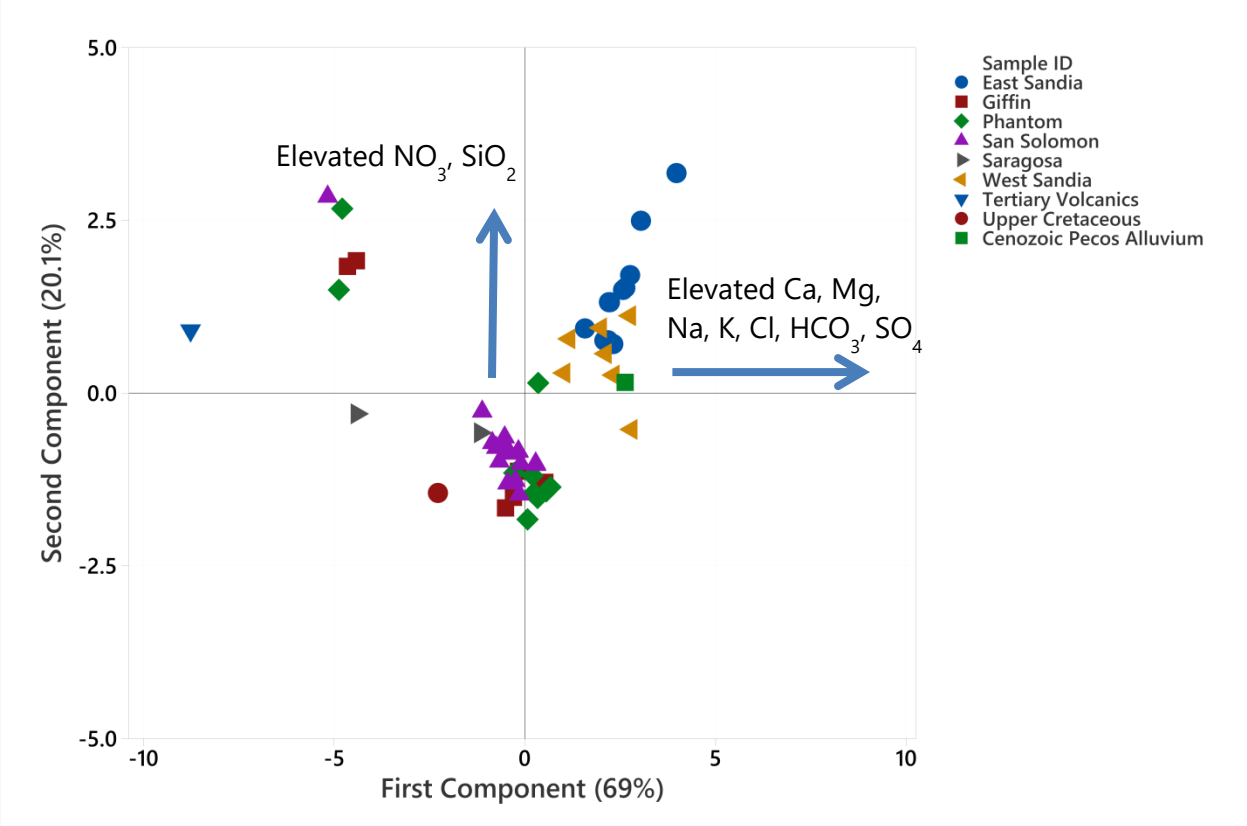

Figure 25. Score plot for PCA.

West Sandia Spring, East Sandia Spring, and the Cenozoic Pecos Alluvium are grouped in one cluster in the score plot (Figure 25). Most of the records for Phantom Lake, San Solomon, and Giffin springs are grouped in a second cluster. One of the two records for Saragosa Spring plots

with this artesian spring cluster, and the other Saragosa record appears as an outlier. PCA also generates a distinct cluster (i.e., upper left quadrant) that represents Phantom Lake Spring, Giffin Spring and San Solomon Spring measurements in 1990 and 2004. The Tertiary Volcanics well plots similarly with these 1990 and 2004 samples. As supported by Appendix B, the samples in the upper left quadrant of Figure 25 are characterized by distinctly low TDS and ion concentrations but elevated in NO_3^- and SiO_2.

EFA was performed using the same variables as the PCA. EFA is simply a PCA with rotation. Factor 1 has the greatest influence and large positive loadings for all of the major ions except NO_3^- and SiO_2 (Table 4). Factor 2 strongly influences NO_3^- and SiO_2 with large negative loadings. Factor 3 is dominated by HCO_3^-. Because HCO_3^- loads heavily on two different factors, it suggests it has more than one process that impacts its distribution.

Overall, the general chemistry of the waters is similar. The first factor loadings close to 1 reflect that because they indicate Factor 1 strongly influences major ion chemistry (i.e., Ca^{2+}, Mg^{2+}, Na^+, K^+, Cl^-, HCO_3^-, SO_4^{2-}). Factor 1 again has large positive loadings on the majors, but HCO_3^- is less correlated to the first factor. Instead, Factor 2 has a strong negative loading on HCO_3^-. Factor 3 has large positive loadings on NO_3^- and SiO_2, although SiO_2 is reduced. EFA suggests HCO_3^-, NO_3^-, and SiO_2 are playing important and about equal roles in this system.

Table 4. Rotated factor loadings using Varimax rotation.

	Variance (%)	Ca^{2+}	Mg^{2+}	Na^+	K^+	Cl^-	HCO_3^-	SO_4^{2-}	NO_3^-	SiO_2
Factor 1	61.9	0.927	0.961	0.955	0.89	0.977	0.47	0.952	-0.028	0.034
Factor 2	12.8	-0.249	-0.149	-0.26	-0.352	-0.172	-0.877	-0.256	0.05	-0.081
Factor 3	11.9	0.134	-0.13	-0.061	-0.076	0.03	-0.048	0.013	0.925	0.409

The score plot of the first two Varimax rotation factors illustrates a similar data structure in comparison to the score plot from PCA, but greater separation and more distinct clusters (Figure 26). The artesian springs have both positive and negative associations with Factor 1, positive associations with Factor 2. The low-TDS records from 1990 and 2004 for the artesian springs have negative associations with Factor 1 and positive associations with Factor 2. Aside from two records for East Sandia Spring, the Cenozoic Pecos Alluvium well, East Sandia Spring, and West Sandia Spring have positive associations with Factor 1 and negative associations with Factor 2. Separation between the rest of the samples and Saragosa Spring is apparent as it has negative associations with both factors.

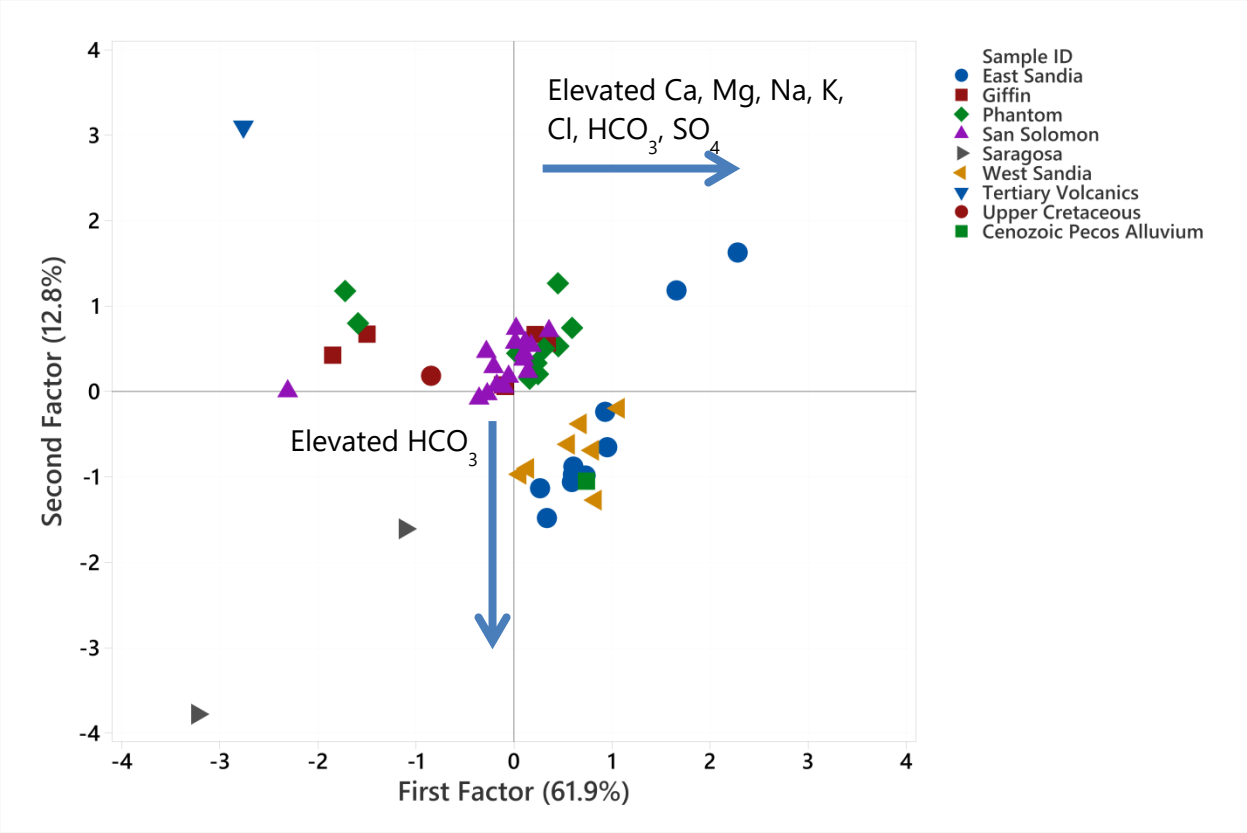

Figure 26. Score plot for EFA.

Discussion

Previous conceptualizations of the regional flow system in Trans-Pecos Texas characterize San Solomon Springs as a multi-outlet spring system and that all outlets have the same local and regional flow components. Seemingly similar hydrochemical assemblages in all six springs may justify this. Despite dominant Na-Cl-SO_4 compositions in all six springs, bivariate plots of ion chemistry and isotopic compositions and multivariate statistical analyses support the notion that there are four different flow components that contribute to the springs: i) the main component is regional flow through carbonate rocks that upwell through the Edwards-Trinity Aquifer and Cenozoic Pecos Alluvium at the springs; (ii) infiltration through the Cenozoic Pecos Alluvium that is added by either irrigation return flow or precipitation and recharges East Sandia and West Sandia springs; (iii) an irrigation or precipitation component near Saragosa Spring contributes to its springflow; and (iv) local precipitation enters the regional system and discharges at the springs.

Source area #1: Regional flow system

Results from this study confirm that Phantom Lake, San Solomon, and Giffin springs are predominantly fed by regional flow paths that emanate from carbonates in the Edwards-Trinity Aquifer. The ion concentrations of the artesian springs group cluster closely and consistently together, which supports the interpretation of a regional and steady contribution identified in previous studies (LaFave and Sharp, 1987; Uliana et al., 2007). Results of this study suggest the regional flow system also contributes to the discharge of East Sandia and West Sandia springs. The potential for interformational flow between the Edwards-Trinity and Pecos Valley Alluvial aquifers has been previously documented (LaFave, 1987, Ashworth, 1990; Jones, 2004). It is conceptualized that the regional flow paths emanating from the Edwards-Trinity Aquifer upwell through the Cenozoic Pecos Alluvium to discharge at East Sandia and West Sandia springs.

The waters of the artesian springs and East Sandia and West Sandia springs are difficult to separate based on hydrochemical assemblages. Oxygen and hydrogen isotopes of these five springs fall along the GMWL, and their $\delta^{18}O$ isotopic signals are suggestive of older waters from a cooler Pleistocene climate. ^{3}H in these five springs indicates recharge waters are submodern. Under perceived baseflow conditions, $\delta^{13}C$ signatures in the five springs are heavy compared to $\delta^{13}C$ signatures of -15‰ typically retained by soils (Chowdhury et al., 2004). Moreover, $\delta^{13}C$ becomes heavier as ^{14}C decreases, which indicates these waters have had sufficient time to interact with the carbonate matrix and retain evolved carbon signatures. High $^{87}Sr/^{86}Sr$ values for the springs are consistent with strontium isotopic signatures from the Wild Horse Flat, which supports a regional flow contribution.

In both PCA and EFA, variables representing major ions tend to load into similar components or factors. This is reasonable given the strong similarities in the major ion chemistry of all spring

samples as illustrated in the Piper diagram (Figure 11). This is also consistent with the conceptualization that the regional groundwater flow system is a significant contributor of flow to most of the six springs. However, PCA and EFA effectively identify clusters of spring hydrochemistry data and other components that highlight differences among the springs.

Major ion chemistry, saturation indices, and carbon isotopes support the interpretation that regional flow upwells through the Cenozoic Pecos Alluvium and ultimately discharges at East Sandia and West Sandia springs. Elevated SiO_2 concentrations in the East Sandia and West Sandia springs are likely derived from upwelling through the alluvial sediments. This also accounts for amorphous silica saturation indices that progress towards equilibrium more so than San Solomon, Phantom Lake, and Giffin springs. Upwelling through and interactions with the alluvial sediments may also contribute to an overall increase in ion concentrations observed in the Sandia springs.

Source area #2: Surface infiltration in the alluvium

Carbon isotope values also suggest that East Sandia and West Sandia springs are fed by local recharge through the Cenozoic Pecos Alluvium. $\delta^{13}C$ and ^{14}C provide a strong basis to surmise that local effects are indeed observed in these samples. In Figure 20, the distinct cluster of $\delta^{13}C$ and ^{14}C for East Sandia and West Sandia springs and the Cenozoic Pecos Alluvium well seemingly appear to be outliers, but interactions with water from recent infiltration that dilutes the older $\delta^{13}C$ signals from regional flow paths may account for this deviation. With respect to ^{3}H and ^{14}C, the infiltration rate of local recharge is much slower than the rain-influenced local recharge to the artesian springs (indicated by elevated ^{3}H with respect to ^{14}C in Figure 21. As a result, ^{3}H relative to the blue mixing line is diminished in East Sandia Spring, West Sandia Spring, and the Cenozoic Pecos Alluvium well due to decay. ^{14}C for these respective ^{3}H compositions should be higher, but ^{14}C is artificially low due to the addition of old carbon from regional flow paths.

In addition to upwelling through the Cenozoic Pecos Alluvium, elevated specific conductivity in the East Sandia and West Sandia springs could also be derived from the addition and recirculation of waters by irrigation return flow that already have high dissolved ion compositions. East Sandia and West Sandia springs appear to have more variability in geochemical behavior than other springs. These may reflect deviations from baseflow conditions that vary with irrigation water type and frequency, although these potential variations of irrigation return flow are not identified or quantified at this time.

NO_3^- is an important component that suggests irrigation return flow impacts East Sandia and West Sandia Springs. NO_3^- concentrations in San Solomon, Phantom Lake, and Giffin Springs are significantly lower than the Sandia springs and are likely background concentrations. East Sandia and West Sandia Springs are downgradient from and proximal to irrigated croplands. These

croplands are likely the source of elevated NO_3^- in East Sandia and West Sandia springs. $\delta^{18}O$ and $\delta^{2}H$ collected in tandem with these NO_3^- measurements suggest some form of irrigation from older waters (and not modern rainfall) provides elevated NO_3^- to the springs. Conversely, the artesian springs are upgradient from irrigated croplands in the area and are likely not impacted.

Source area #3: Near-surface flow to Saragosa Spring

Data from this study suggest that a near-surface component provides for the distinct hydrochemical assemblage of Saragosa Spring. Ionic compositions in Saragosa Spring discharge are comparable to those of the artesian springs, although EFA clearly segregates Saragosa Spring based on its ion chemistry. Impacts to Saragosa Spring from a shallow surface environment and a low-flow component are indicated by highly variable temperatures. It is important to note that these temperature variations cannot be used to ascertain the source of flow to Saragosa Spring. However, $\delta^{2}H$ and $\delta^{18}O$ plot along the GMWL and alongside the Tertiary Volcanics well and GNIP station, which are representative of modern rainfall in the region. ^{14}C and ^{3}H confirm the contribution of modern to sub-modern water. The nearness of Saragosa Spring discharge to the surface indicates much younger water is mixing with its springflow, which would ultimately produce smaller $\delta^{13}C$ values and elevated ^{3}H and ^{14}C. The strontium ion concentration and isotopic signal are preferentially diluted in Saragosa Spring with respect to the other sample sites but are still elevated in comparison to waters from the Davis Mountains and surrounding carbonates. This may suggest that there are contributions from modern irrigation or volcanics derived water (which has lower Sr and lower $^{87}Sr/^{86}Sr$). The near-surface component or mechanism that gives Saragosa Spring a different geochemical signature likely suggests that Saragosa Spring is a seepage spring (i.e., where groundwater slowly seeps out of the ground) in the alluvium.

Source area #4: Local precipitation

This study confirms that local flow from precipitation events impacts all springs in the San Solomon Springs system. The 1990 and 2004 measurements for San Solomon, Phantom Lake, and Giffin springs that cluster separately in PCA and EFA score plots support a hydrologic response to rain events that differs from baseflow conditions. These clusters are located in the score plots in the same direction as the Tertiary Volcanics well, which is what would be expected if these waters are modern. Deviations from baseflow conditions due to a rain event include elevated ^{3}H signals.

East Sandia Spring was also sampled during the 2004 synoptic water quality sampling event. Although this 2004 record does not fall within the PCA clusters of low-TDS artesian springs, East Sandia Spring counterintuitively responds to this speculated rain event with elevated ion concentrations and lighter $\delta^{13}C$. This 2004 record, along with a second sample collected two

months prior, deviates from clusters identified in the score plots. Chowdhury et al. (2004) ascertained that East Sandia Spring is hydraulically connected to the artesian springs, so all four springs responding to speculated rain events may further support this hydraulic connection. This temporal component could be explored further with additional sampling after rain events to better understand why East Sandia Spring has a counterintuitive hydraulic response.

Limitations

Major ion chemistry and isotopic analytical results from the September-October 2020 sampling campaign were not received in time to be included in this report. The hydraulic response of West Sandia and Saragosa springs to precipitation/recharge events has not yet been documented, so their hydraulic connection to the other springs has not been determined. There are limited records for San Solomon Springs hydrochemistry used in multivariate statistical analyses. Namely, there are less than 10 hydrochemical records each for West Sandia Spring and Saragosa Spring included in this study. Additional sampling of the springs, with emphasis on data collection from West Sandia and Saragosa springs should enable a better understanding of characteristic hydrochemistry. ^{14}C data for East Sandia and West Sandia springs and the Cenozoic Pecos Alluvium wells are also limited; additional samples should be collected from these locations to evaluate if elevated modern carbon signatures in these springs are persistent or ephemeral.

This study is limited to 14 records of boron isotope data, namely two $\delta^{11}B$ measurements for each spring and one $\delta^{11}B$ measurement for the Cenozoic Pecos Alluvium and Upper Cretaceous wells. Dissolved boron in the Tertiary Volcanics well sample was below the detection threshold to provide a viable analytical result. Boron isotopic data for host rocks and groundwaters in the study area are not documented in the literature. Characteristic boron concentrations and isotopic signatures of groundwater affected by irrigation return flow or anthropogenic contamination are not identified at this time. However, the mixing line between San Solomon Spring and the Cenozoic Pecos Alluvium well for $\delta^{11}B$ may indicate a mixing trend between the regional flow paths that upwell through the alluvial sediments. It is possible that the alluvium has higher boron content than the surrounding carbonates. Regional flow paths that ultimately discharge at East Sandia and West Sandia springs may pick up elevated boron concentrations and isotopic signals by upwelling through the alluvial sediments. Potential mixing provides support to further examine the hydraulic communication between the different flow components using $\delta^{11}B$.

Samples were not collected from the Rustler Formation and Permian carbonates and evaporites upgradient of the springs to better constrain endmembers or isotopic behavior (e.g., $\delta^{11}B$) identified in San Solomon Springs. Moreover, the Upper Cretaceous, Cenozoic Pecos Alluvium and Tertiary Volcanics wells sampled may not be fully representative of endmembers in the

system. For example, the Upper Cretaceous well water may be different from Edwards-Trinity Aquifer water used for irrigation. However, these water sample results do provide a guide for general chemistries of different waters in the region.

Conclusions and future work

San Solomon Springs in Trans-Pecos Texas provides an example of a multi-outlet, multi-source spring system. San Solomon Springs consists of San Solomon, Phantom Lake, Giffin, East Sandia, West Sandia, and Saragosa springs. Collectively, the springs provide habitats for federally endangered and endemic species and are used to meet irrigation, recreation, and municipal needs. Effective water management requires that the different flow components that contribute to spring discharge at San Solomon Springs be understood well enough to assess impacts of changes in recharge and/or groundwater withdrawals.

Geochemical and statistical analyses of these samples provide insight into hydraulic relationships among the springs. Samples from each spring and surrounding wells in the Upper Cretaceous, Cenozoic Pecos Alluvium, and Tertiary Volcanics were collected and analyzed for major ion chemistry and isotopic compositions. Groundwater in all of the springs and wells is characterized by mineralized flow. Trilinear diagrams indicate similar spring water chemistry, and geochemical equilibria suggest water-rock interactions with carbonate, evaporite, and siliciclastic rocks. Ionic and isotopic compositions of San Solomon, Phantom Lake, Giffin, East Sandia, and West Sandia springs support the conceptualization that groundwater recharged during a cooler and wetter climate (i.e., during the Pleistocene). These regional flow paths emanate from the Edwards-Trinity Aquifer to directly feed San Solomon, Phantom Lake, and Giffin springs. These same flow regional paths contribute to East Sandia and West Sandia springs from the Edwards-Trinity Aquifer by upwelling through the Cenozoic Pecos Alluvium. Elevated ion concentrations and nutrient compositions suggest irrigation return flow may be a source of local recharge to East Sandia and West Sandia springs. Conversely, evidence for Saragosa Spring hydrochemical uniqueness is strong, as isotopic compositions suggests modern waters provide recharge and contribute to its characterization as a seepage spring.

Variations in hydrochemistry are related to mechanisms and locations of recharge. Using ion chemistry alone, PCA and EFA clusters fall into the four flow components that contribute to San Solomon Springs. Isotopic compositions provide evidence to further support the conceptualization of a combination of local and regional flow to the springs. The four flow components to San Solomon Springs include: (i) a main component of regional flow through carbonate rocks that upwell through the Edwards-Trinity Aquifer and Cenozoic Pecos Alluvium at the springs; (ii) infiltration through the Cenozoic Pecos Alluvium that is added by either irrigation return flow or precipitation and recharges East Sandia and West Sandia springs; (iii) an irrigation or precipitation component near Saragosa Spring that contributes to its springflow; and (iv) local precipitation enters the regional system and discharges at the springs.

Future work will include additional sampling funded by internal research grants from Southwest Research Institute, multivariate techniques, and geochemical modeling to prove or disprove that

differences between the artesian and gravity springs are persistent and not ephemeral. Future field investigations will emphasize the collection of water samples for multi-isotope analysis to better constrain the interpretations of source areas to the springs. This revised approach will incorporate $\delta^{15}N\text{-}NO_3$ and $\delta^{18}O\text{-}NO_3$ to provide greater insight regarding elevated nitrate concentrations in East Sandia and West Sandia springs. This may provide a means to constrain potential contributions from irrigation return flow that potentially capture an anthropogenic signal (e.g., fertilizers).

Fifteen percent ($6,859 of the $45,000 awarded) of the project funds remain as of December 29, 2020. The remaining funds will be used to support future data analysis and interpretation. Once additional datasets are available from the September 2020 field campaign, the remainder of project funds from Big Bend Conservation Alliance will provide refined conceptualizations of the different local and regional flow contributions to San Solomon Springs. The project will be completed and the final report will be submitted by May 14, 2021.

Appendix A: Field parameters

Table A 1: Field parameters of the San Solomon Springs system and surrounding wells.

Sample Name	Date	pH	Temperature (°C)	DIC	Specific Conductivity (µS/cm)	DO (mg/L)	Field alkalinity (mg/L as $CaCO_3$)
East Sandia	6/7/2004	6.80	20.5		5020	3.03	212
East Sandia	8/4/2004	6.90	20.3		4730	2.2	224
East Sandia	2/27/2019*	6.96	18.3		4400	5.10	
East Sandia	5/28/2019	7.00	19.4		2890		292
East Sandia	12/5/2019*	6.81	20.1	65.1	3687	7.50	259
East Sandia	9/30/2020*	6.96	19.9		4011	6.16	248
Giffin	11/1/1990	6.90	22.8		1550		176
Giffin	6/7/2004	7.10	25.1		3420	1.87	205
Giffin	8/4/2004	7.20	24.8		1918	3.5	174
Giffin	2/27/2019*	7.29	24.5		3600	3.87	
Giffin	12/6/2019*	6.95	25.0	51.9	3773	4.40	200
Giffin	9/30/2020*	7.17	25.8		3274	5.18	204
Phantom	10/31/1990	7.30	22.5		1530		166
Phantom	6/11/2001	7.10	25.3		3560	1.4	217
Phantom	7/25/2003	7.20	25.4		3500		226
Phantom	8/3/2004	7.20	23.5		1786	3.45	169
Phantom	2/26/2019*	7.04	24.1		3800	1.79	
San Solomon	4/14/1990	7.30	26				
San Solomon	11/1/1990	7.20	20.8		1298		186
San Solomon	6/12/2001	7.00	25.5		3420		220
San Solomon	6/8/2004	7.20	25.1		3430	3.12	206
San Solomon	8/4/2004	7.10	24.4		3080	2.4	209
San Solomon	4/22/2015	7.10	25.6		3230		226
San Solomon	2/27/2019*	6.98	22.7		3200	3.63	
San Solomon	5/28/2019	7.30	24.4		2470		235
San Solomon	12/5/2019*	6.91	24.6	52.8	3057	3.27	204
San Solomon	10/1/2020*	6.97	24.8		3363	2.49	198
Saragosa	2/27/2019*	7.38	13.0		2500	6.73	
Saragosa	12/6/2019*	7.16	11.9	70.3			275
Saragosa	9/30/2020*	7.44	26.2		3420	4.67	226
West Sandia	2/26/2019*	7.06	20.8		4100	3.84	
West Sandia	12/5/2019*	6.71	21.9	61.2	3407	5.18	247
West Sandia	9/30/2020*	7.06	19.6		3763	1.69	289
Tertiary Volcanics	12/5/2019*	7.21	19.9	24	208	7.90	83
Upper Cretaceous	12/6/2019*	6.91	25.8	50.3	3020	7.10	201
Cenozoic Pecos Alluvium	12/5/2019*	6.80	22.0	66.6	3831	4.00	253

*Field parameters collected during this study. Other records are from TPWD (2019) and TWDB (2019).

Table B 1: Ion concentrations of San Solomon Springs and surrounding wells.

Sample Name	Date	Ca^{2+} (mg/L)	Mg^{2+} (mg/L)	Na^{+} (mg/L)	K^{+} (mg/L)	Cl^{-} (mg/L)	HCO_3^{-} (mg/L)	SO_4^{2-} (mg/L)	NO_3^{-} (mg/L)	Sr^{2+} (µg/L)	B^{3+} (µg/L)
East Sandia	6/7/2004	340	105	611	24	1050	276	978	8.51	5080	245
East Sandia	8/4/2004	303	96	584	24	916	284	891	6.33	5010	
East Sandia	6/26/2017	243	86	540	23	770	342	878	3.62	4040	425
East Sandia	12/12/2017	243	84	565	26	844	325	872	4.19	4170	356
East Sandia	3/5/2018	244	87	570	26	857	334	880	5.89	4530	439
East Sandia	6/11/2018	256	89	553	24	804	348	829	4.32	4370	424
East Sandia	9/17/2018	244	82	571	23	765	342	823	3.71	3980	399
East Sandia	12/10/2018	229	79	553	23	811	344	864	4.52	3890	364
East Sandia	2/27/2019	249	82	500	24	733	355	788	3.63	3800	336
East Sandia	5/28/2019	255	87	502	24	773	338	795	4.36	4230	460
East Sandia	12/5/2019	230	80	481	22	697	340	810	3.92	3860	368
Giffin	5/29/1990	186	79	463	25	628	276	679	0.89	3830	680
Giffin	11/1/1990	114	30	166	13	245	233	269	7.17	1720	200
Giffin	6/7/2004	179	78	440	19	638	268	665	0.83	3190	219
Giffin	8/4/2004	114	40	207	10	305	225	323	8.37	1850	
Giffin	2/27/2019	191	77	398	21	561	283	592	0.78	3230	269
Giffin	12/6/2019	177	75	398	19	579	281	610	0.55	3260	289
Phantom Lake	10/31/1990	105	30	163	13	247	210	267	6.11	1730	180
Phantom Lake	6/11/2001	175	80	418	22	664	273	463	1.04	3430	391
Phantom Lake	7/25/2003	180	81	456	21	660	276	680	0.97	3440	277
Phantom Lake	8/3/2004	109	37	189	9	281	216	299	10.23	1640	
Phantom Lake	6/28/2017	182	81	437	21	627	282	645	0.71	3410	358
Phantom Lake	12/13/2017	183	80	456	22	674	264	705	0.77	3390	273
Phantom Lake	2/28/2018	189	85	485	22	695	271	728	1.10	3610	337
Phantom Lake	6/12/2018	185	82	445	22	630	281	654	0.62	3450	363
Phantom Lake	2/26/2019	197	85	437	21	605	284	676	0.79	3480	143
Phantom Lake	1/28/2020	199	88	482	22	632	277	666	0.85	3650	306

Table B 1 Continued: Ion concentrations of San Solomon Springs and surrounding wells.

San Solomon	4/14/1990	185	75	440	24	628	284	650	1.24	4300	570
San Solomon	11/1/1990	99	23	133	12	178	248	213	7.30	1350	160
San Solomon	10/15/1998	188	80	441	22	657	271	701	1.05	3610	449
San Solomon	6/12/2001	182	77	392	20	620	272	678	1.08	3200	378
San Solomon	6/8/2004	182	80	445	19	615	273	641	0.97	3140	219
San Solomon	8/4/2004	163	68	384	17	555	267	569	2.17	3010	
San Solomon	4/22/2015	183	78	407	19	571	265	593	1.32	3280	224
San Solomon	1/26/2017	171	69	394	18	577	284	595	1.65	2980	
San Solomon	1/27/2017	171	69	389	18	550	285	567	1.61	2975	
San Solomon	12/12/2017	176	73	391	20	614	268	632	1.35	3140	260
San Solomon	3/6/2018	179	76	416	20	627	275	646	1.51	3520	338
San Solomon	6/12/2018	179	76	402	20	554	283	573	1.69	3210	326
San Solomon	9/18/2018	185	77	387	20	519	276	541	1.04	3300	315
San Solomon	2/27/2019	195	78	389	21	556	284	588	1.03	3320	264
San Solomon	5/28/2019	189	80	419	20	567	275	651	0.97	3470	376
San Solomon	12/5/2019	178	76	402	19	600	278	607	1.22	3230	302
Saragosa	2/27/2019	175	60	330	19	417	331	507	1.15	2680	210
Saragosa	12/6/2019	81	24	172	12	146	375	201	0.04	1210	171
West Sandia	6/26/2017	249	91	508	25	809	328	831	4.14	4090	389
West Sandia	12/12/2017	243	89	549	27	843	347	871	3.56	4250	315
West Sandia	3/6/2018	244	93	545	26	831	321	911	4.70	4480	431
West Sandia	6/12/2018	236	88	510	25	716	329	806	3.71	4150	
West Sandia	9/18/2018	237	83	541	25	742	325	850	2.56	3960	410
West Sandia	2/26/2019	223	79	449	24	669	327	705	4.40	3500	322
West Sandia	12/5/2019	214	79	446	23	665	331	713	2.78	3540	356
Tertiary Volcanics	12/5/2019	31	3	13	2	4	127	5	2.46	86	
Upper Cretaceous	12/6/2019	155	59	306	14	461	265	455	0.12	2630	214
Cenozoic Pecos Alluvium	12/5/2019	233	92	596	26	774	347	808	2.71	4190	385

Appendix C: Isotopic compositions

Table C 1. Isotopic compositions of San Solomon Springs and surrounding wells.

Spring Name	Date	$\delta^{2}H$ (‰ VSMOW)	$\delta^{18}O$ (‰ VSMOW)	$\delta^{13}C$ (‰ PDB)	$\delta^{11}B$ (‰ NIST SRM 951a)	^{3}H (TU)	$^{87}Sr/^{86}Sr$
East Sandia	5/29/1998						0.709683
East Sandia	6/7/2004	-59.50	-8.54				
East Sandia	8/4/2004	-66.00	-8.50	-12.30		0.55	
East Sandia	2/24/2019	-53.03	-8.07	-9.17	14.4	0.39	0.7097079
East Sandia	12/5/2019	-57.85	-8.28	-8.90	16.1	0.50	0.709688
East Sandia	9/30/2020				14.8		
Giffin	5/29/1998						0.709999
Giffin	6/7/2004	-62.20	-9.13				
Giffin	8/4/2004	-63.00	-8.10	-10.70		1.38	
Giffin	2/24/2019	-64.15	-8.78	-6.31	10.0	0.04	0.709962
Giffin	12/6/2019	-61.98	-8.94	-6.30	11.0	-0.03	0.709976
Giffin	9/30/2020				12.5		
Phantom Lake	3/28/1998						0.710007
Phantom Lake	6/11/2001	-65.00	-9.25	-7.40		0.06	
Phantom Lake	3/3/2003						
Phantom Lake	6/7/2004	-63.30	-9.18				
Phantom Lake	8/3/2004	-61.00	-8.00	-11.4		1.53	
Phantom Lake	2/23/2019	-61.37	-8.82	-6.30	10.7	-0.09	0.7099869
Phantom Lake	1/28/2020	-70.12	-10.07	-6.00	14.6	0.07	0.709994
San Solomon	2/23/2019	-63.29	-8.67	-6.69	8.0	0.84	0.7099122
San Solomon	12/5/2019	-61.65	-8.87	-6.90	9.6	0.02	0.709967
San Solomon	10/1/2020				15.2		
San Solomon	3/27/1998						0.709991
San Solomon	6/12/2001	-68.50	-9.10	-7.30		0.17	
San Solomon	3/3/2003						
San Solomon	6/8/2004	-63.10	-9.14				
San Solomon	8/4/2004	-66.00	-8.70	-9.90		0.63	
Saragosa	2/24/2019	-48.68	-7.14	-9.86	17.0	1.31	0.7095254
Saragosa	12/6/2019	-48.09	-6.99	-13.40	12.4	2.66	0.709478
Saragosa	9/30/2020				16.2		
West Sandia	2/23/2019	-57.45	-8.16	-9.10	12.9	0.11	0.709788
West Sandia	12/5/2019	-59.75	-8.54	-9.10	12.4	0.21	0.709775
West Sandia	9/30/2020				13.7		
Tertiary Volcanics	12/5/2019	-48.51	-7.14	-12.90		0.63	0.707782
Upper Cretaceous	12/6/2019	-58.66	-8.56	-7.20	15.9	0.21	0.709816
Cenozoic Pecos Alluvium	12/5/2019	-61.51	-8.72	-8.70	17.8	0.32	0.709903

References

Ashworth, J.B. (1990). Evaluation of ground-water resources in parts of Loving, Pecos, Reeves, Ward, and Winkler counties, Texas. Texas Water Development Board, Report 317, 51 p.

Banner, J.L., and Kaufman, J. (1994). The isotopic record of ocean chemistry and diagenesis preserved in non-luminescent brachiopods from Mississippian carbonate rocks, Illinois and Missouri. Geological Society of America Bulletin, v. 106, p. 1074-1082. https://doi.org/10.1130/0016-7606(1994)106<1074:TIROOC>2.3.CO;2

Bethke, C.M. (2008). Geochemical and Biogeochemical Reaction Modeling. Cambridge University Press, New York, 547 pp.

Bethke, C.M., Farrell, B., and Sharifi, M. (2020). The Geochemist's Workbench® User's Guides, Release 14.0. Aqueous Solutions LLC, Champaign.

Bhandary, H., Al-Senafy, M., and Marzouk, F. (2015). Usage of Carbon Isotopes in Characterizing Groundwater Age, Flow Direction, Flow Velocity and Recharge Area. Procedia Environmental Sciences, v. 25, p. 28-35. https://doi.org/10.1016/j.proenv.2015.04.005

Birk, S., Liedl, R., and Sauter, M. (2004). Identification of localised recharge and conduit flow by combined analysis of hydraulic and physico-chemical spring responses (Urenbrunnen, SW-Germany). Journal of Hydrology, v. 286, 1-4, p. 179-193. https://doi.org/10.1016/j.jhydrol.2003.09.007

Boghici, R. (2003). A Field Manual for Groundwater Sample. Texas Water Development Board, User Manual 51, 47 p.

Boghici, R. and Van Broekhoven, N.G. (2001) Hydrogeology of the Rustler Aquifer, Trans-Pecos Texas. Pages 207–225, in R.E. Mace, W.F. Mullican, III, and E.S. Angle, eds. Aquifers of West Texas. Texas Water Development Board, Austin, Texas, Report 356.

Bro, R., and Smilde, A. (2014) Principal component analysis. Anal. Methods, 6, p. 2812-2831. https://doi.org/10.1039/C3AY41907J

Bullen, T.D., and Kendall, C. (1998). Tracing of Weathering Reactions and Water Flowpaths: A Multi-isotope Approach In C. Kendall and J. J. McDonnell (Eds.), Isotope Tracers in Catchment Hydrology. Elsevier, pp. 611-646. https://doi.org/10.1016/B978-0-444-81546-0.50025-2

Bumgarner, J.R., Stanton, G.P., Teeple, A.P., Thomas, J.V., Houston, N.A., Payne, J.D., and Musgrove, M. (2012). A Conceptual Model of the Hydrogeologic Framework, Geochemistry, and Groundwater-Flow System of the Edwards-Trinity and Related Aquifers in the Pecos County Region, Texas. U.S. Geological Survey Scientific Investigations Report 2012-5124, 74 p. https://doi.org/10.3133/sir20125124

Chowdhury, A.H., Ridgeway, C., and Mace, R.E. (2004). Origin of the waters in the San Solomon Spring system, Trans-Pecos Texas, *in* R.E. Mace, E.S. Angle, and W.F. Mullican, III, eds. Aquifers of the Edwards Plateau. Texas Water Development Board, Report 360, pp. 315–344.

Clark, I. and D. and Fritz, P. (1997). Environmental isotopes in Hydrogeology, Lewis Publishers, 328 p.

Cook, P. (2020). Introduction to isotopes and environmental tracers as indicators of groundwater flow. The Groundwater Project, 84 p.

Couch, H.E. (1978). Study of the lower Cretaceous and associated aquifers in the Balmorhea district of Trans-Pecos, Texas. Department of Water Resources, Report, 61 p.

Craig, H. (1961). Isotopic Variations in Meteoric Waters: Science, v. 133, p. 1702-1703. https://doi.org/10.1126/science.133.3465.1702

Davidson, G.R., and Bassett, R.L. (1993). Application of boron isotopes for identifying contaminants such as fly ash leachate in groundwater. Environmental Science and Technology, vol. 27, no. 1, p. 172-176. https://doi.org/10.1021/es00038a020

Doctor, D.H., Alexander, E.C., Petrič, M., Kogovšek, J., Urbanc, J., Lojen, S., and Stichler, W. (2006). Quantification of karst aquifer discharge components during storm events through end-member mixing analysis using natural chemistry and stable isotopes as tracers. Hydrogeology Journal, v. 14, p. 1171-1191. https://doi.org/10.1007/s10040-006-0031-6

Foster, G., Lécuyer, C., and Marschall, H. (2016). Boron Stable Isotopes. In: White W. (eds) Encyclopedia of Geochemistry. Encyclopedia of Earth Sciences Series. Springer, Cham. https://doi.org/10.1007/978-3-319-39193-9_238-1

Hem, J.D. (1982). Study and interpretation of chemical characteristics of natural water. U.S. Geological Survey Water-Supply Paper 2254, 272 p.

Hiss, W. L. (1980). Movement of groundwater in Permian Guadalupian aquifer systems, southeastern New Mexico and Western Texas *in* Dickerson, P. W., and Hoffer, J. M., eds., Trans-Pecos region. New Mexico Geological Society, 31st Field Conference Guidebook, Trans-Pecos Region, p. 289-294.

Huebsch, M., Fenton, O., Horan, B., Hennessy, D., Richards, K.G., Jordan, P., Goldscheider, N., Butscher, C., and Blum, P. (2014). Mobilisation or dilution? Nitrate response of karst springs to high rainfall events. Hydrology and Earth System Sciences, v. 18, p. 4423-4435. https://doi.org/10.5194/hessd-11-4131-2014

International Atomic Energy Agency (IAEA) (1981). Statistical treatment of environmental isotope data in precipitation. Technical Report Series No. 206.

Jones, I.C. (2004). Cenozoic Pecos Alluvium Aquifer, in Mace, R.E., Angle, E.S., and Mullican, W.F., III, eds., Aquifers of the Edwards Plateau. Texas Water Development Board, Report 360, p. 142-164.

Kendall, C., Caldwell, E.A., and Snyder, D. (2005). Resources on isotopes—Periodic table—Boron. U.S. Geological Survey Isotope Tracers Project: accessed November 14, 2020, at http://wwwrcamnl.wr.usgs.gov/isoig/period/b_iig.html.

Knierim, K.J., Pollock, E., and Hays, P.D. (2013). Using isotopes of dissolved inorganic carbon species and water to separate sources of recharge in a cave spring, Northwestern Arkansas, USA. Acta Carsologica, v. 42, p. 261-276. https://doi.org/10.3986/ac.v42i2-3.667

LaFave, J.I. (1987). Groundwater flow delineation in the Toyah Basin of Trans-Pecos Texas. The University of Texas at Austin, Master's Thesis, 159 p., 1 plate.

LaFave, J. I. and Sharp Jr., J. M. (1987). Origins of groundwater discharging at the springs of Balmorhea. West Texas Geological Society Bulletin, v. 26, pp. 5-14.

Mance, D., Hunjak, T., Lenac, D., Rubinić, J., and Roller-Lutz, Z. (2014). Stable isotope analysis of the karst hydrological systems in the Bay of Kvarner (Croatia). Applied Radiation and Isotopes, v. 90, p. 23-34. https://doi.org/10.1016/j.apradiso.2014.03.001

Minitab 19 Statistical Software (2019). [Computer software]. State College, PA: Minitab, Inc. (www.minitab.com).

Muehlberger, W. R., and Dickerson, P. W. (1989). A tectonic history of Trans-Pecos Texas. In Dickerson, P. W., Hoffer, J. M., and Callender, J. F. (Eds.), *New Mexico Geological Society 31stst Annual Field Conference Guidebook*, p. 35-54. https://doi.org/10.1029/FT317p0035

Nimz, G. J. (1998). Lithogenic and Cosmogenic Tracers in Catchment Hydrology. In: C. Kendall and J. J. McDonnell (Eds.), *Isotope Tracers in Catchment Hydrology*. Elsevier, pp. 247-290. https://doi.org/10.1016/B978-0-444-81546-0.50015-X

Parkhurst, D.L., and Appelo, C.A.J. (2013). Description of input and examples for PHREEQC version 3—A computer program for speciation, batch-reaction, one-dimensional transport, and

inverse geochemical calculations. U.S. Geological Survey Techniques and Methods, Book 6, Chap. A43, 497 p. http://doi.org/10.3133/tm6a43.

Pennisi, M., Gonfiantini, R., Grassi, S., and Squarci, P. (2006). The utilization of boron and strontium isotopes for the assessment of boron contamination of the Cecina River alluvial aquifer (central-western Tuscany, Italy). Applied Geochemistry, v. 21, p. 643-655. https://doi.org/10.1016/j.apgeochem.2005.11.005

Piper, A.M. (1944). A graphic procedure in the geochemical interpretation of water analyses. American Geophysical Union Transactions, v. 25, p. 914-923. https://doi.org/10.1029/TR025i006p00914

Ravbar, N., Engelhardt, I., and Goldscheider, N. (2011). Anomalous behavior of specific electrical conductivity at a karst spring induced by variable catchment boundaries: the case of the Podstenjšek spring, Slovenia. Hydrological Processes, v.25, p. 2130-2140, https://doi.org/10.1002/hyp.7966.

Ridgeway C, Austin B, Boghici R, Chowdhury A, Christian B, Coker D, Mace R, Mathews R, Schuster S, Smith R, and Watson W. (2005). Diminished spring flows in the San Solomon Springs System, Trans-Pecos, Texas. Texas Parks and Wildlife Report 84312 [unpublished]. https://tpwd.texas.gov/business/grants/wildlife/section6/docs/habitats/e19_final_report.pdf.

Robertson, W.M., Allen, J.T., Wolaver, B.D., and Sharp Jr., J.M. (2019). Aridland spring response to mesoscale precipitation: Implications for groundwater-dependent ecosystem sustainability. Journal of Hydrology, 570, p. 850-862. https://doi.org/10.1016/j.jhydrol.2018.12.074

Sharp, J.M., Jr., (1990). Regional groundwater system in northern Trans-Pecos Texas: in Kreitler, C.W., and Sharp, J.M., Hydrogeology of Trans-Pecos Texas. The University of Texas at Austin, Bureau of Economic Geology, Guidebook 25, p. 113-120.

TPWD, 2019, Spring water chemistry data: personal communication from Chad Norris and Marty Kelly (TPWD) via email dated March 5, 2019.

TWDB, 2019, Groundwater database download: website http://www.twdb.texas.gov/groundwater/data/gwdbrpt.asp, accessed August 2019.

Uliana, M.M. (2000). Delineation of regional groundwater flow paths and their relation to the structural features in the Salt and Toyah basins. The University of Texas at Austin, Ph.D. Dissertation, 131 p.

Uliana, M.M., Banner, J.L., and Sharp Jr., J.M. (2007). Regional groundwater flow paths in Trans-Pecos, Texas inferred from oxygen, hydrogen, and strontium isotopes. Journal of Hydrology, v. 334, p. 334-346, https://doi.org/10.1016/j.jhydrol.2006.10.015.

Veale, N., Visser, A., Esser, B., Singleton, M.J., and Moran, J.E. (2019). Nitrogen Cycle Dynamics Revealed Through $\delta^{18}O\text{-}NO_3$ – Analysis on California Groundwater. Geosciences, v. 9, 15 p. https://doi.org/10.3390/geosciences9020095

Vengosh, A., Heumann, K.G., Juraske, S., Kasher, R. (1994). Boron Isotope Application for Tracing Sources of Contamination in Groundwater. Environmental Science & Technology, v.28, p. 1968-1974. https://doi.org/10.1021/es00060a030

White, W. N., Gale, H. S., and Nye, S. S. (1941). Geology and ground-water resources of the Balmorhea area, western Texas. Geological Survey Water-Supply Paper, (849-C). https://doi.org/10.3133/wsp849C

Zhang, Y., Shi, P., Song, J., and Li, Q. (2019). Application of Nitrogen and Oxygen Isotopes for Source and Fate Identification of Nitrate Pollution in Surface Water. A Review, Applied Science, v. 9, 18 p. https://doi.org/10.3390/app9010018